Investigations of Zeros near the Central Point of Elliptic Curve L-Functions

Steven J. Miller, with an appendix by Eduardo Dueñez

CONTENTS

We explore the effect of zeros at the central point on nearby zeros of elliptic-curve L-functions, especially for one-parameter families of rank r over $\mathbb{Q}$. By the Birch and Swinnerton-Dyer conjecture and Silverman's specialization theorem, for t sufficiently large the L-function of each curve E_t in the family has r zeros (called the family zeros) at the central point. We observe experimentally a repulsion of the zeros near the central point, and the repulsion increases with r. There is greater repulsion in the subset of curves of rank $r+2$ than in the subset of curves of rank r in a rank-r family. For curves with comparable conductors, the behavior of rank-2 curves in a rank-0 one-parameter family over $\mathbb{Q}$ is statistically different from that of rank-2 curves from a rank-2 family. In contrast to excess-rank calculations, the repulsion decreases markedly as the conductors increase, and we conjecture that the r family zeros do not repel in the limit. Finally, the differences between adjacent normalized zeros near the central point are statistically independent of the repulsion, family rank, and rank of the curves in the subset. Specifically, the differences between adjacent normalized zeros are statistically equal for all curves investigated with rank 0, 2, or 4 and comparable conductors from one-parameter families of rank 0 or 2 over $\mathbb{Q}$.

1. INTRODUCTION

Random-matrix theory has successfully modeled the behavior of the zeros and values of many L-functions; see, for example, the excellent surveys [Keating and Snaith 03, Farmer 05]. The correspondence first appeared in Montgomery's analysis of the pair correlation[1] of the zeros of the Riemann zeta function as the zeros tend to

[1] If $\{\alpha_j\}_{j=1}^{\infty}$ is an increasing sequence of numbers and $B \subset \mathbb{R}^{n-1}$ is a compact box, the n-level correlations are

$$\lim_{N\to\infty} \# \frac{\{(\alpha_{j_1}-\alpha_{j_2},\dots,\alpha_{j_{n-1}}-\alpha_{j_n}) \in B, j_i \le N, j_i \ne j_k\}}{N}.$$

One may replace the boxes with smooth test functions; see [Rudnick and Sarnak 96] for details.

2000 AMS Subject Classification: Primary 11M26; Secondary 11G05, 11G40, 11M26

Keywords: Elliptic curves, low-lying zeros, n-level statistics, random-matrix theory

1058-6458/2006 $ 0.50 per page

infinity [Montgomery 73]. Dyson noticed that Montgomery's answer, though limited to test functions satisfying certain support restrictions, agrees with the pair correlation of the eigenvalues from the Gaussian unitary ensemble (GUE).[2] Montgomery conjectured that his result holds for all correlations and all support. Again with suitable restrictions and in the limit as the zeros tend to infinity, Hejhal [Hejhal 94] showed that the triple correlation of zeros of the Riemann zeta function agrees with the GUE, and more generally, Rudnick and Sarnak [Rudnick and Sarnak 96] showed that the n-level correlations of the zeros of any principal L-function (the L-function attached to a cuspidal automorphic representation of GL_m over $\mathbb{Q}$) also agree with the GUE.

In this paper we explore another connection between L-functions and random-matrix theory: the effect of multiple zeros at the central point on nearby zeros of an L-function and the effect of multiple eigenvalues at 1 on nearby eigenvalues in a classical compact group. Particularly interesting cases are families of elliptic-curve L-functions. It is conjectured that zeros of primitive L-functions are simple, except potentially at the central point for arithmetic reasons. For an elliptic curve E, the Birch and Swinnerton-Dyer conjecture [Birch and Swinnerton-Dyer 63, Birch and Swinnerton-Dyer 65] states that the rank of the Mordell–Weil group $E(\mathbb{Q})$ equals the order of vanishing of the L-function $L(E,s)$ at the central point $s = \frac{1}{2}$.[3] Let $\mathcal{E}$ be a one-parameter family of elliptic curves over $\mathbb{Q}$ with (Mordell–Weil) rank r:[4]

$$y^2 = x^3 + A(T)x + B(T), \quad A(T), B(T) \in \mathbb{Z}[T]. \quad (1\text{–}1)$$

For all t sufficiently large, each curve E_t in the family $\mathcal{E}$ has rank at least r, by Silverman's specialization theorem [Silverman 94]. Thus we expect each curve's L-function to have at least r zeros at the central point. We call the r conjectured zeros from the Birch and Swinnerton-Dyer conjecture the *family zeros*. Thus, at least conjecturally, these families of elliptic curves offer an exciting and accessible laboratory in which we can explore the effect of multiple zeros on nearby zeros.

The main tool for studying zeros near the central point (the *low-lying zeros*) in a family is the n-level density. Let $\phi(x) = \prod_{i=1}^n \phi_i(x_i)$, where the ϕ_i are even Schwartz functions whose Fourier transforms $\widehat{\phi_i}$ are compactly supported. Following [Iwaniec et al. 00], we define the n-level density for the zeros of an L-function $L(s,f)$ by

$$D_{n,f}(\phi) = \sum_{\substack{j_1,\dots,j_n \\ j_k \neq \pm j_\ell}} \phi_1\left(\gamma_{f,j_1}\frac{\log C_f}{2\pi}\right)\cdots\phi_n\left(\gamma_{f,j_n}\frac{\log C_f}{2\pi}\right), \quad (1\text{–}2)$$

where C_f is the analytic conductor of $L(s,f)$, whose nontrivial zeros are $\frac{1}{2}+i\gamma_{f,j}$. Under the generalized Riemann hypothesis (GRH), the nontrivial zeros all lie on the critical line $\Re(s) = \frac{1}{2}$, and thus $\gamma_{f,j} \in \mathbb{R}$. Since ϕ_i is Schwartz, note that most of the contribution is from zeros near the central point. The analytic conductor of an L-function normalizes the nontrivial zeros of the L-function so that near the central point, the average spacing between normalized zeros is 1; it is determined by analyzing the Γ-factors in the functional equation of the L-function (see, for example, [Iwaniec et al. 00]). For elliptic curves the analytic conductor is the conductor of the elliptic curve (the level of the corresponding weight-2 cuspidal newform from the modularity theorem of [Wiles 95, Taylor and Wiles 95, Breuil et al. 01]).

We order a family $\mathcal{F}$ of L-functions by analytic conductors. Let $\mathcal{F}_N = \{f \in \mathcal{F} : C_f \leq N\}$. The n-level density for the family $\mathcal{F}$ with test function ϕ is

$$D_{n,\mathcal{F}}(\phi) = \lim_{N\to\infty} D_{n,\mathcal{F}_N}(\phi), \quad (1\text{–}3)$$

where

$$D_{n,\mathcal{F}_N} = \frac{1}{|\mathcal{F}_N|}\sum_{f\in\mathcal{F}_N} D_{n,f}(\phi). \quad (1\text{–}4)$$

We can of course investigate other subsets. Other common choices are $\{f : C_f \in [N,2N]\}$ and, for a one-parameter family $\mathcal{E}$ of elliptic curves over $\mathbb{Q}$, $\{E_t \in \mathcal{E} : t \in [N,2N]\}$.

Let $\mathrm{U}(N)$ be the ensemble of $N \times N$ unitary matrices with Haar measure. The classical compact groups are subensembles $G(N)$ of $\mathrm{U}(N)$; the most frequently encountered ones are $\mathrm{USp}(2M)$, $\mathrm{SO}(2N)$, and $\mathrm{SO}(2N+1)$. Katz and Sarnak's density conjecture [Katz and Sarnak 99a, Katz and Sarnak 99b] states that as the conductors tend to infinity, the behavior of the normalized zeros near the central point equals the $N \to \infty$ scaling limit of the normalized eigenvalues near 1 of a classical compact group; see (1–7) for an exact statement. In the function-field case, the corresponding classical compact group can be identified from the monodromy group; in the number-field case, however, the reason behind the

---

[2] The GUE is the $N \to \infty$ scaling limit of $N \times N$ complex Hermitian matrices with entries independently chosen from Gaussians; see [Mehta 91] for details.

[3] We normalize all L-functions to have functional equation $s \mapsto 1-s$, and thus the central point is at $s = \frac{1}{2}$.

[4] The group of rational function solutions $(x(T), y(T)) \in \mathbb{Q}(T)^2$ to $y^2 = x^3 + A(T)x + B(T)$ is isomorphic to $\mathbb{Z}^r \oplus \mathbb{T}$, where $\mathbb{T}$ is the torsion part and r is the rank.

identification is often a mystery (see [Dueñez and Miller 06]). Since the eigenvalues of a unitary matrix are of the form $e^{i\theta}$, we often talk about the eigenangles θ instead of the eigenvalues $e^{i\theta}$, and the eigenangle 0 corresponds to the eigenvalue 1.

Using the explicit formula we replace the sums over zeros in (1–2) with sums over the Fourier coefficients at prime powers. For example, if $E : y^2 = x^3 + Ax + B$ is an elliptic curve, then assuming GRH, the nontrivial zeros of the associated L-function

$$L(E, s) = \sum_{n=1}^{\infty} \lambda_E(n) n^{-s} \tag{1–5}$$

(normalized to have functional equation $s \mapsto 1 - s$) are $\frac{1}{2} + i\gamma$, $\gamma \in \mathbb{R}$. If ϕ is a Schwartz test function, then the explicit formula for $L(E, s)$ is

$$\begin{aligned} &\sum_{\gamma_j} \phi\left(\gamma_j \frac{\log C_E}{2\pi}\right) \qquad (1\text{–}6) \\ &= \widehat{\phi}(0) + \phi(0) - 2\sum_p \frac{\log p}{\log C_E} \widehat{\phi}\left(\frac{\log p}{\log C_E}\right) \frac{\lambda_E(p)}{\sqrt{p}} \\ &\quad - 2\sum_p \frac{\log p}{\log C_E} \widehat{\phi}\left(\frac{2\log p}{\log C_E}\right) \frac{\lambda_E^2(p)}{p} + O\left(\frac{\log\log C_E}{\log C_E}\right); \end{aligned}$$

see, for example, [Mestre 86, Miller 02]. Using appropriate averaging formulas and combinatorics, the resulting prime-power sums in the n-level densities can be evaluated for $\widehat{\phi}_i$ of suitably restricted support. The density conjecture is that for each family of L-functions $\mathcal{F}$, for any Schwartz test function $\phi : \mathbb{R}^n \to \mathbb{R}^n$,

$$D_{n,\mathcal{F}}(\phi) = \int \phi(x) W_{n,\mathcal{G}}(x)\, dx = \int \widehat{\phi}(u) \widehat{W}_{n,\mathcal{G}}(u)\, du. \tag{1–7}$$

The density kernel $W_{n,\mathcal{G}}(x)$ is determined from the $N \to \infty$ scaling limit of the associated classical compact group $G(N)$; the last equality follows by Plancherel. The most frequently occurring answers are the scaling limits of unitary, symplectic, and orthogonal ensembles. For $n = 1$ we have

$$\begin{aligned} \widehat{W}_{1,\mathrm{U}}(u) &= \delta(u), \\ \widehat{W}_{1,\mathrm{USp}}(u) &= \delta(u) - \frac{1}{2}\mathrm{I}(u), \\ \widehat{W}_{1,\mathrm{SO(even)}}(u) &= \delta(u) + \frac{1}{2}\mathrm{I}(u), \\ \widehat{W}_{1,\mathrm{SO(odd)}}(u) &= \delta(u) - \frac{1}{2}\mathrm{I}(u) + 1, \\ \widehat{W}_{1,\mathrm{O}}(u) &= \delta(u) + \frac{1}{2}, \end{aligned} \tag{1–8}$$

where $\mathrm{I}(u)$ is the characteristic function of $[-1, 1]$. For arbitrarily small support, unitary and symplectic are distinguishable from each other and the orthogonal groups; however, for test functions $\widehat{\phi}$ supported in $(-1, 1)$, the three orthogonal groups agree:

$$\begin{aligned} \int \widehat{\phi}(u) \widehat{W}_{1,\mathrm{U}}(u)\, du &= \widehat{\phi}(u), \\ \int \widehat{\phi}(u) \widehat{W}_{1,\mathrm{USp}}(u)\, du &= \widehat{\phi}(u) - \frac{1}{2}\phi(0), \\ \int \widehat{\phi}(u) \widehat{W}_{1,\mathrm{SO(even)}}(u)\, du &= \widehat{\phi}(u) + \frac{1}{2}\phi(0), \\ \int \widehat{\phi}(u) \widehat{W}_{1,\mathrm{SO(odd)}}(u)\, du &= \widehat{\phi}(u) + \frac{1}{2}\phi(0), \\ \int \widehat{\phi}(u) \widehat{W}_{1,\mathrm{O}}(u)\, du &= \widehat{\phi}(u) + \frac{1}{2}\phi(0). \end{aligned} \tag{1–9}$$

Similar results hold for the n-level densities, but below we need only the 1-level density; see [Conrey 05, Katz and Sarnak 99a] for the derivations of the general n-level densities, and Appendix A for the 1-level density for the orthogonal groups.

For one-parameter families of elliptic curves, the results suggest that the correct models are orthogonal groups (if all functional equations are even then the answer is SO(even), while if all are odd the answer is SO(odd)). Often, instead of normalizing each curve's zeros by the logarithm of its conductor (the local rescaling), one instead uses the average log-conductor (the global rescaling). If we are interested in only the average rank, it suffices to study just the 1-level density from the global rescaling. This is because we care only about the imaginary parts of the zeros at the central point, and both scalings of the imaginary part of the central point are zero; see, for example, [Brumer 92, Goldfeld 79, Heath-Brown 04, Michel 95, Silverman 98, Young 06]. To date, all results have support in $(-1, 1)$, where (1–9) shows that the behavior of O, SO(even), and SO(odd) are indistinguishable. If we want to specify a unique corresponding classical compact group, we study the 2-level density as well, which for arbitrarily small support suffices to distinguish the three orthogonal candidates. Using the global rescaling removes many complications in the 1-level sums but not in the 2-level sums. In fact, for the 2-level investigations the global rescaling is as difficult as the local rescaling; see [Miller 04] for details.

Our research was motivated by investigations into the distribution of rank in families of elliptic curves as the conductors grow. As we see below, for the ranges of conductors studied there is poor agreement between elliptic-curve-rank data and the $N \to \infty$ scaling limits of random-matrix theory. The purpose of this research is to show that another statistic, the distribution of the first few zeros above the central point, converges more rapidly.

We briefly review the excess-rank phenomenon. A generic one-parameter family of elliptic curves over $\mathbb{Q}$ has half of its functional equations even and half odd (see [Helfgott 04] for the precise conditions for a family to be generic). Consider such a one-parameter family of elliptic curves over $\mathbb{Q}$, of rank r, and assume the Birch and Swinnerton-Dyer conjecture. It is believed that the behavior of the nonfamily zeros is modeled by the $N \to \infty$ scaling limit of orthogonal matrices. Thus if the density conjecture is correct, then at the central point in the limit as the conductors tend to infinity, the L-functions have exactly r zeros 50% of the time, and exactly $r+1$ zeros 50% of the time. Thus in the limit, half the curves have rank r and half have rank $r+1$. In a variety of families, however, one observes[5] that 30% to 40% have rank r, about 48% have rank $r+1$, 10% to 20% have rank $r+2$, and about 2% have rank $r+3$; see, for example, [Brumer and McGuinness 91, Fermigier 92, Fermigier 96, Zagier and Kramarz 87].

We give a representative family below; see in particular [Fermigier 96] for more examples. Consider the one-parameter family $y^2 = x^3 + 16Tx + 32$ of rank 0 over $\mathbb{Q}$. Each range in the table below has 2000 curves (the run time in the last column is in hours):

T-range	rank 0	rank 1	rank 2	rank 3	run time
$[-1000, 1000)$	39.4%	47.8%	12.3%	0.6%	< 1
$[1000, 3000)$	38.4%	47.3%	13.6%	0.6%	< 1
$[4000, 6000)$	37.4%	47.8%	13.7%	1.1%	1
$[8000, 10000)$	37.3%	48.8%	12.9%	1.0%	2.5
$[24000, 26000)$	35.1%	50.1%	13.9%	0.8%	6.8
$[50000, 52000)$	36.7%	48.3%	13.8%	1.2%	51.8

The relative stability of the percentage of curves in a family rank 2 above the family with rank r naturally leads to the question whether this persists in the limit; it cannot persist if the density conjecture (with orthogonal groups) is true for all support.[6] Recently, Watkins [Watkins 04] investigated the family $x^3 + y^3 = m$ for varying m, and in contrast to other families, his range of m was large enough to see the percentage with rank $r+2$ markedly decrease, providing support for the density conjecture (with orthogonal groups).

In our example above, as well as in the other families investigated, the logarithms of the conductors are quite small. Even in our last set the log-conductors are under 40. An analysis of the error terms in the explicit formula suggests that the rate of convergence of quantities related to zeros of elliptic curves is like the logarithm of the conductors. It is quite satisfying when we study the first few normalized zeros above the central point to see that in contrast to excess rank, we see a dramatic decrease in repulsion with modest increases in conductor.

In Section 2 we study two random-matrix ensembles that are natural candidates to model families of elliptic curves with positive rank. Many natural questions concerning the normalized eigenvalues for these models for finite N lead to quantities that are expressed in terms of eigenvalues of integral equations. Our hope is that showing the possible connections between these models and number theory will spur interest in studying these models and analyzing these integral equations. We assume the Birch and Swinnerton-Dyer conjecture, as well as GRH. We calculate some properties of these ensembles in Appendix A.

In Section 3 we summarize the theoretical results of previous investigations, which state the following:

- For one-parameter families of rank r over $\mathbb{Q}$ and suitably restricted test functions, as the conductors tend to infinity the 1-level densities imply that in this restricted range, the r family zeros at the central point are independent of the remaining zeros.

If this were to hold for all test functions, then as the conductors tend to infinity the distribution of the first few normalized zeros above the central point would be independent of the r family zeros.

In Section 4 we numerically investigate the first few normalized zeros above the central point for elliptic curves from many families of different rank. Our main observations are these:

- The first few normalized zeros are repelled from the central point. The repulsion increases with the number of zeros at the central point, and even in the case in which there are no zeros at the central point there is repulsion from the large-conductor-limit theoretical prediction. This is observed for the family of

[5] Actually, this is not quite true. The analytic rank is estimated by the location of the first nonzero term in the series expansion of $L(E,s)$ at the central point (see [Cremona 92] for the algorithms). For example, if the zeroth through third coefficients are smaller than 10^{-5} and the fourth is 1.701, then we say that the curve has analytic rank 4, even though it is possible (though unlikely) that one of the first four coefficients is really nonzero. It is difficult to prove that an elliptic-curve L-function vanishes to order two or greater. [Goldfeld 76] and [Gross and Zagier 87] give an effective lower bound for the class number of imaginary quadratic fields by an analysis of an elliptic-curve L-function that is proven to have three zeros at the central point.

[6] Explicitly, if the large-conductor limits of the elliptic-curve L-functions agree with the $N \to \infty$ scaling limits of orthogonal groups.

all elliptic curves, and for one-parameter families of rank r over $\mathbb{Q}$.

- There is *greater* repulsion in the first normalized zero above the central point for subsets of curves of rank 2 from one-parameter families of rank 0 over $\mathbb{Q}$ than for subsets of curves of rank 2 from one-parameter families of rank 2 over $\mathbb{Q}$. It is conjectured that as the conductors tend to infinity, 0% of curves in a family of rank r have rank $r + 2$ or greater. If this is true, we are comparing a subset of zero relative measure to one of positive measure. Since the first set is (conjecturally) so small, it is not surprising that to date there is no known theoretical agreement with any random-matrix model for this case.

- In contrast to most excess-rank investigations, as the conductors increase, the repulsion of the first few normalized zeros markedly decreases. This supports the conjecture that in the limit as the conductors tend to infinity, the family zeros are independent of the remaining normalized zeros (i.e., the repulsion from the family zeros vanishes in the limit).

- The repulsion from additional zeros at the central point cannot entirely be explained by collapsing some zeros to the central point and leaving all the other zeros alone. See in particular Remark 4.5.

- While the first few normalized zeros are repelled from the central point, the *differences* between normalized zeros near the central point are statistically independent of the repulsion as well as the method of construction. Specifically, the differences between adjacent zeros near the central point from curves of rank 0, 2, or 4 with comparable conductors from one-parameter families of rank 0 or 2 over $\mathbb{Q}$ are statistically equal. Thus the data suggest that the effect of the repulsion is simply to shift all zeros by approximately the same amount.

The numerical data are similar to those in excess-rank investigations. While both seem to contradict the density conjecture, the density conjecture describes the limiting behavior as the conductors tend to infinity. The rate of convergence is expected to be on the order of the logarithms of the conductors, which is under 40 for our curves. Thus our experimental results are likely misleading as to the limiting behavior. It is quite interesting that in contrast to most excess-rank investigations, we can easily go far enough to see conductor-dependent behavior.

Thus our theoretical and numerical results, as well as the Birch and Swinnerton-Dyer and density conjectures, lead us to the following conjecture:

Conjecture 1.1. *Consider one-parameter families of elliptic curves of rank r over $\mathbb{Q}$ and their subfamilies of curves with rank exactly $r + k$ for $k \in \{0, 1, 2, \dots\}$. For each subfamily there are r family zeros at the central point, and these zeros repel the nearby normalized zeros. The repulsion increases with r and decreases to zero as the conductors tend to infinity, implying that in the limit the r family zeros are independent of the remaining zeros. If $k \geq 2$, these additional nonfamily zeros at the central point may influence nearby zeros, even in the limit as the conductors tend to infinity. The spacings between adjacent normalized zeros above the central point are independent of the repulsion; in particular, it does not depend on r or k, but only on the conductors.*

2. RANDOM-MATRIX MODELS FOR FAMILIES OF ELLIPTIC CURVES

We want a random-matrix model for the behavior of zeros from families of elliptic-curve L-functions with a prescribed number of zeros at the central point. We concentrate on models for either one- or two-parameter families over $\mathbb{Q}$, and refer the reader to [Farmer 05] for more on random-matrix models. Both of these families are expected to have orthogonal symmetries. Many researchers (see, for example, [David et al. 04, Goldfeld 79, Gouvéa and Mazur 91, Mai 93, Rubin and Silverberg 01, Rubinstein 01, Stewart and Top 95]) have studied families constructed by twisting a fixed elliptic curve by characters. The general belief is that such twisting should lead to unitary or symplectic families, depending on the orders of the characters.

There are two natural models for the corresponding situation in random-matrix theory of a prescribed number of eigenvalues at 1 in subensembles of orthogonal groups. For ease of presentation we consider the case of an even number of eigenvalues at 1; the odd case is handled similarly.

Consider a matrix in $\mathrm{SO}(2N)$. It has $2N$ eigenvalues in pairs $e^{\pm i\theta_j}$, with $\theta_j \in [0, \pi]$. The joint probability measure on $\Theta = (\theta_1, \dots, \theta_N) \in [0, \pi]^N$ is

$$d\epsilon_0(\Theta) = c_N \prod_{1 \leq j < k \leq N} (\cos\theta_k - \cos\theta_j)^2 \prod_{1 \leq j \leq N} d\theta_j, \quad (2–1)$$

where c_N is a normalization constant such that $d\epsilon_0(\Theta)$ integrates to 1. From (2–1) we can derive all quantities of interest on the random-matrix side; in particular, n-level densities, distribution of first normalized eigenvalue above 1 (or eigenangle above 0), and so forth.

We now consider two models for subensembles of $\mathrm{SO}(2N)$ with $2r$ eigenvalues at 1, and the $N \to \infty$ scaling limit of each.

Independent Model: The subensemble of $\mathrm{SO}(2N)$ with the upper left block a $2r \times 2r$ identity matrix. The joint probability density of the remaining $N - r$ pairs is given by

$$d\varepsilon_{2r,\mathrm{Indep}}(\Theta) = c_{2r,\mathrm{Indep},N} \prod_{1 \le j < k \le N-r} (\cos\theta_k - \cos\theta_j)^2 \times \prod_{1 \le j \le N-r} d\theta_j. \quad (2\text{–}2)$$

Thus the ensemble is matrices of the form

$$\left\{ \begin{pmatrix} I_{2r\times 2r} & \\ & g \end{pmatrix} : g \in \mathrm{SO}(2N-2r) \right\}; \quad (2\text{–}3)$$

the probabilities are equivalent to choosing g with respect to Haar measure on $\mathrm{SO}(2N-2r)$. We call this the independent model, since the forced eigenvalues at 1 from the $I_{2r\times 2r}$ block do not interact with the eigenvalues of g. In particular, the distribution of the remaining $N - r$ pairs of eigenvalues is exactly that of $\mathrm{SO}(2N - 2r)$; this block's $N \to \infty$ scaling limit is just SO(even). See [Conrey 05, Katz and Sarnak 99a] as well as Appendix A.

Interaction Model: The subensemble of $\mathrm{SO}(2N)$ with $2r$ of the $2N$ eigenvalues equaling 1:

$$d\varepsilon_{2r,\mathrm{Inter}}(\Theta) = c_{2r,\mathrm{Inter},N} \prod_{1 \le j < k \le N-r} (\cos\theta_k - \cos\theta_j)^2 \times \prod_{1 \le j \le N-r} (1-\cos\theta_j)^{2r} d\theta_j. \quad (2\text{–}4)$$

We call this the interaction model because the forced eigenvalues at 1 *do* affect the behavior of the other eigenvalues near 1. Note here that we condition on all $\mathrm{SO}(2N)$ matrices with at least $2r$ eigenvalues equal to 1. The $(1 - \cos\theta_j)^{2r}$ factor results in the forced eigenvalues at 1 repelling the nearby eigenvalues.

Remark 2.1. Since the calculations for the local statistics near the eigenvalue at 1 in the interaction model have not appeared in print, Appendix A (written by Eduardo Dueñez) provides a derivation of formula (2–4) (see especially Section A.2), as well as the relevant integral (Bessel) kernels dictating such statistics. See also [Snaith 05] for the value distribution of the first nonzero derivative of the characteristic polynomials of this ensemble.

While both models have at least $2r$ eigenvalues equal to 1, they are very different subensembles of $\mathrm{SO}(2N)$, and they have distinct limiting behavior (see also Remark 3.1). We can see this by computing the 1-level density for each, and comparing with (1–9). Letting $\widehat{W}_{1,\mathrm{SO(even)}}$ (respectively $\widehat{W}_{1,\mathrm{SO(even)},\mathrm{Indep},2r}$ and $\widehat{W}_{1,\mathrm{SO(even)},\mathrm{Inter},2r}$) denote the Fourier transform of the kernel for the 1-level density of SO(even) (respectively, of the independent model for the subensemble of SO(even) with $2r$ eigenvalues at 1 and of the interaction model for the subensemble of SO(even) with $2r$ eigenvalues at 1), we find in Appendix A that

$$\begin{aligned} \widehat{W}_{1,\mathrm{SO(even)}}(u) &= \delta(u) + \frac{1}{2}\mathrm{I}(u), \\ \widehat{W}_{1,\mathrm{SO(even)},\mathrm{Indep},2r}(u) &= \delta(u) + \frac{1}{2}\mathrm{I}(u) + 2, \\ \widehat{W}_{1,\mathrm{SO(even)},\mathrm{Inter},2r}(u) &= \delta(u) + \frac{1}{2}\mathrm{I}(u) + 2 \\ &\quad + 2(|u|-1)\mathrm{I}(u). \end{aligned} \quad (2\text{–}5)$$

Since $\mathrm{I}(u)$ is positive for $|u| < 1$, note that the density is smaller for $|u| < 1$ in the interaction model versus the independent model. We can interpret this as a repulsion of zeros, as the following heuristic shows (though see Appendix A for proofs). We compare the 1-level density of zeros from curves with and without repulsion, and show that for a positive decreasing test function, the 1-level density is smaller when there is repulsion.

Consider two elliptic curves, E of rank 0 and conductor C_E and E' of rank r and conductor $C_{E'}$. Assume $C_E \approx C_{E'} \approx C$, and assume GRH for both L-functions. If the curve E has rank 0 then we expect the first zero above the central point, $\frac{1}{2} + i\gamma_{E,1}$, to have $\gamma_{E,1} \approx \frac{1}{\log C}$. For E_r, if the r family zeros at the central point repel, it is reasonable to posit a repulsion of size $\frac{b_r}{\log C}$ for some $b_r > 0$. This is because the natural scale for the distance between the low-lying zeros is $\frac{1}{\log C}$, so we are merely positing that the repulsion is proportional to the distance. We assume that all zeros are repelled equally; evidence for this is provided in Section 4.6. Thus for E' (the repulsion case) we assume $\gamma_{E',j} \approx \gamma_{E,j} + \frac{b_r}{\log C}$. We can detect this repulsion by comparing the 1-level densities of E and E'. Take a nonnegative decreasing Schwartz test function ϕ. The difference between the contribution from the jth zero of each is

$$\begin{aligned}\phi\left(\gamma_{E',j}\frac{\log C}{2\pi}\right) - \phi\left(\gamma_{E,j}\frac{\log C}{2\pi}\right) \\ \approx \phi\left(\gamma_{E,j}\frac{\log C}{2\pi} + \frac{b_r}{2\pi}\right) - \phi\left(\gamma_{E,j}\frac{\log C}{2\pi}\right) \\ \approx \phi'\left(\gamma_{E,j}\frac{\log C}{2\pi}\right)\cdot\frac{b_r}{2\pi}.\end{aligned} \tag{2–6}$$

Since $\widehat{\phi}$ is decreasing, its derivative is negative and thus the above shows that the 1-level density for the zeros from E' (assuming repulsion) is smaller than the 1-level density for zeros from E. Thus the lower 1-level density in the interaction model versus the independent model can be interpreted as a repulsion; however, this repulsion can be shared among several zeros near the central point. In fact, the observations in Section 4.6 suggest that the repulsion shifts all normalized zeros near the central point approximately equally.

3. THEORETICAL RESULTS

Consider a one-parameter family of elliptic curves of rank r over $\mathbb{Q}$. We summarize previous investigations of the effect of the (conjectured) r family zeros on the other zeros near the central point. For convenience we state the results for the global rescaling, though similar results hold for the local rescaling (under slightly more restrictive conditions; see [Miller 04] for details). For small support, the 1- and 2-level densities agree with the scaling limits of

$$\begin{pmatrix} I_{r\times r} & \\ & \mathrm{O}(N) \end{pmatrix}, \qquad \begin{pmatrix} I_{r\times r} & \\ & \mathrm{SO}(2N) \end{pmatrix},$$

and

$$\begin{pmatrix} I_{r\times r} & \\ & \mathrm{SO}(2N+1) \end{pmatrix},$$

depending on whether the signs of the functional equation are equidistributed or all the signs are even or all the signs are odd. The 1- and 2-level densities provide evidence in support of the Katz–Sarnak density conjecture for test functions whose Fourier transforms have small support (the support is computable and depends on the family). See [Miller 02] for the calculations with the global rescaling, though the result for the 1-level density is implicit in [Silverman 98]. Similar results are observed for two-parameter families of elliptic curves in [Miller 02, Young 06].

While the above results are consistent with the Birch and Swinnerton-Dyer conjecture that each curve's L-function has at least r zeros at the central point, it is not a proof (even in the limit) because our supports are finite. For families with $t \in [N, 2N]$ the errors are of size $O(\frac{1}{\log N})$ or $O(\frac{\log\log N}{\log N})$. Thus for large N we cannot distinguish a family with exactly r zeros at the central point from a family in which each E_t has exactly r zeros at $\pm(\log C_t)^{-2006}$.

For one-parameter families of elliptic curves over $\mathbb{Q}$, in the limit as the conductors tend to infinity the family zeros (those arising from our belief in the Birch and Swinnerton-Dyer conjecture) appear to be independent of the other zeros. Equivalently, if we remove the contributions from the r family zeros, for test functions with suitably restricted support the spacing statistics of the remaining zeros agree perfectly with the standard orthogonal groups O, SO(even), and SO(odd), and it is conjectured that these results should hold for all support. Thus the n-level density arguments support the independent over the interaction model when we study *all* curves in a family; however, these theoretical arguments do not apply if we study the subfamily of curves of rank $r+k$ ($k \geq 2$) in a rank-r one-parameter family over $\mathbb{Q}$.

Remark 3.1. It is important to note that our theoretical results are for the entire one-parameter family. Specifically, consider the subset of curves of rank $r+2$ from a one-parameter family of rank r over $\mathbb{Q}$. If the density conjecture (with orthogonal groups) is true, then in the limit, 0% of curves are in this subfamily. Thus these curves may behave differently without contradicting the theoretical results for the entire family. Situations in which the behavior of subensembles is different from that of the entire ensemble are well known in random-matrix theory. For example, to any simple graph we may attach a real symmetric matrix, its adjacency matrix, for which $a_{ij} = 1$ if there is an edge connecting vertices i and j, and 0 otherwise. The adjacency matrices of d-regular graphs are a thin subensemble of real symmetric matrices with entries independently chosen from $\{-1, 0, 1\}$. The densities of normalized eigenvalues in the two cases are quite different, given by Kesten's measure [McKay 81] for d-regular graphs and Wigner's semicircle law [Mehta 91] for the real symmetric matrices.

It is an interesting question to determine the appropriate random-matrix model for rank-$(r+2)$ curves in a rank-r one-parameter family over $\mathbb{Q}$, both in the limit of large conductors as well as for finite conductors. We explore this issue in greater detail in Sections 4.3 through 4.6, where we compare the behavior of rank-2 curves from rank-0 one-parameter families over $\mathbb{Q}$ to that of rank-2 curves from rank-2 one-parameter families over $\mathbb{Q}$.

4. EXPERIMENTAL RESULTS

We investigate the first few normalized zeros above the central point. We used Michael Rubinstein's L-function calculator [Rubinstein 05] to determine the zeros. The program does a contour integral to ensure that we have found all the zeros in a region, which is essential in studies of the first zero! See [Rubinstein 98] for a description of the algorithms. The analytic ranks were found (see Footnote 1) by determining the values of the L-functions and their derivatives at the central point by the standard series expansion; see [Cremona 92] for the algorithms. Some of the programs and all of the data (minimal model, conductor, discriminant, sign of the functional equation, first nonzero Taylor coefficient from the series expansion at the central point, and the first three zeros above the central point) are available online at http://www.math.brown.edu/∼sjmiller/repulsion.

We study several one-parameter families of elliptic curves over $\mathbb{Q}$. Since all of our families are rational surfaces,[7] Rosen and Silverman's result that the weighted average of fibral Frobenius trace values determines the rank over $\mathbb{Q}$ (see [Rosen and Silverman 98]) is applicable, and evaluating simple Legendre sums suffices to determine the rank. We mostly use one-parameter families from Fermigier's tables [Fermigier 96], though see [Arms et al. 06] for how to use the results of [Rosen and Silverman 98] to construct additional one-parameter families with rank over $\mathbb{Q}$.

We cannot obtain a decent number of curves with approximately equal log-conductors by considering a solitary one-parameter family. The conductors in a family typically grow polynomially in t. The number of Fourier coefficients needed to study a value of $L(s, E_t)$ on the critical line is of order $\sqrt{C_t}\log C_t$ (C_t is the conductor of E_t), and we must then additionally evaluate numerous special functions. We can readily calculate the needed quantities up to conductors of size 10^{11}, which usually translates to just a few curves in a family. We first studied all elliptic curves (parameterized with more than one parameter), found the minimal models, and then sorted by conductor. We then studied several one-parameter families, amalgamating data from different families if the curves had the same rank and similar log-conductor.

[7] An elliptic surface $y^2 = x^3 + A(T)x + B(T)$, $A(T), B(T) \in \mathbb{Z}[T]$, is a rational surface if and only if one of the following is true: (a) $0 < \max\{3\deg A, 2\deg B\} < 12$; (b) $3\deg A = 2\deg B = 12$ and $\mathrm{ord}_{T=0}T^{12}\Delta(T^{-1}) = 0$.

Remark 4.1. Amalgamating data from different one-parameter families warrants some discussion. We expect that the behavior of zeros from curves with similar conductors and the same number of zeros and family zeros at the central point should be approximately equal. In other words, we hope that curves with the same rank and approximately equal conductors from different one-parameter families of the same rank r over $\mathbb{Q}$ behave similarly, and we may regard the different one-parameter families of rank r over $\mathbb{Q}$ as different measurements of this universal behavior. This is similar to numerical investigations of the spacings of energy levels of heavy nuclei; see, for example, [Harvey and Hughes 58, Haq et al. 82]. In studying the spacings of these energy levels, there were very few (typically between 10 and 100) levels for each nucleus. The belief is that nuclei with the same angular momentum and parity should behave similarly. The resulting amalgamations often have thousands of spacings and excellent agreement with random-matrix predictions.

As with the excess-rank phenomenon, we found disagreement between the experiments and the predicted large-conductor limit; however, we believe that this disagreement is due to the fact that the logarithms of the conductors investigated are small. In Sections 4.2 through 4.5 we find that for curves with zeros at the central point, the first normalized zero above the central point *is* repelled, and the greater the number of zeros at the central point, the greater the repulsion. However, the repulsion decreases as the conductors increase. Thus the repulsion is probably due to the small conductors, and in the limit the independent model (which agrees with the function-field analogue and the theoretical results of Section 3) should correctly describe the first normalized zero above the central point in curves of rank r in families of rank r over $\mathbb{Q}$. It is not known what the correct model is for curves of rank $r + 2$ in a family of rank r over $\mathbb{Q}$, though it is reasonable to conjecture that it is the interaction model with the sizes of the matrices related to the logarithms of the conductors. Keating and Snaith [Keating and Snaith 00, Keating and Snaith 03] showed that to study zeros at height T it is better to look at $N \times N$ matrices, with $N = \log T$, than to look at the $N \to \infty$ scaling limit. A fascinating question is to determine the correct finite-conductor analogue for the two different cases here. Interestingly, we see in Section 4.6 that the spacings between adjacent normalized zeros is statistically independent of the repulsion, which implies that the effect of the zeros at the central point (for finite conductors) is to shift *all* the nearby zeros approximately equally.

4.1 Theoretical Predictions: Independent Model

In Figures 1 and 2 we plot the first normalized eigenangle above 0 for SO($2N$) (i.e., SO(even)) and SO($2N+1$) (i.e., SO(odd)) matrices.

The eigenvalues occur in pairs $e^{\pm i\theta_j}$, $\theta_j \in [0,\pi]$; by normalized eigenangles for SO(even) or SO(odd) we mean $\theta_j \frac{N}{\pi}$. We chose $2N \leq 6$ and $2N+1 = 7$ for our simulations, and chose our matrices with respect to the appropriate Haar measure.[8] We thank Michael Rubinstein for sharing his $N \to \infty$ scaling limit plots for SO($2N$) and SO($2N+1$).

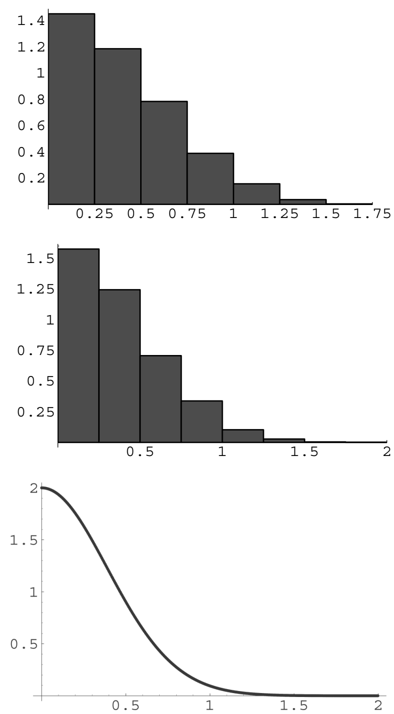

FIGURE 1. Top: First normalized eigenangle above 0: 23,040 SO(4) matrices; mean = .357, standard deviation about the mean = .300, median = .357. Center: First normalized eigenangle above 0: 23,040 SO(6) matrices mean = .325, standard deviation about the man = .284, median = .325. Bottom: First normalized eigenangle above 0: $N \to \infty$ scaling limit of SO($2N$): mean = .321.

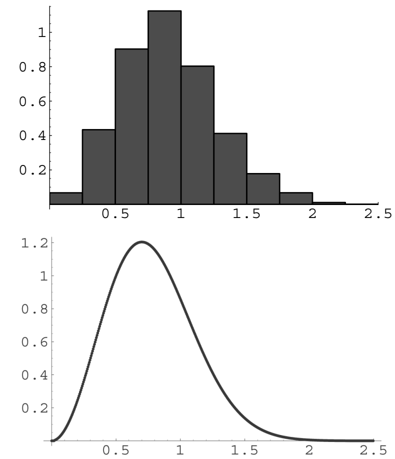

FIGURE 2. Top: First normalized eigenangle above 1: 322,560 SO(7) matrices mean = .881, standard deviation about the mean = .360, median = .881. Bottom: First normalized eigenangle above 1: $N \to \infty$ scaling limit of SO($2N+1$): mean = .782.

For the SO($2N$) matrices, note that the mean decreases as $2N$ increases. A similar result holds for SO($2N+1$) matrices; since we study primarily even rank below, we concentrate on SO($2N$) here. As $N \to \infty$, it is proved in [Katz and Sarnak 99b, pp. 412–415]) that the mean of the first normalized eigenangle above $\theta = 0$ (corresponding to the eigenvalue 1) for SO(even) is approximately 0.321, while for SO(odd) it is approximately 0.782.

We study the first normalized zero above the central point for elliptic-curve L-functions in Sections 4.2 through 4.5. We rescale each zero: $\gamma_{E_t,1} \mapsto \gamma_{E_t,1} \frac{\log C_t}{2\pi}$. The mean of the first normalized eigenangle above 0 for SO($2N$) matrices decreases as $2N$ increases, and similarly we see that the first normalized zero above the central point in families of elliptic curves decreases as the conductor increases. This suggests that a good finite-conductor model for families of elliptic curves with even functional equation and conductors of size C may be SO($2N$), with N some function of $\log C$.

4.2 All Curves

4.2.1 Rank-0 Curves. We study the first normalized zero above the central point for 1500 rank-0 elliptic curves, 750 with log(cond) $\in [3.2, 12.6]$ in Figure 3 and 750 with log(cond) $\in [12.6, 14.9]$ in Figure 4. These curves were obtained as follows: an elliptic curve can be written in Weierstrass form as

$$y^2 + a_1xy + a_3y = x^3 + a_2x^2 + a_4x + a_6, \quad a_i \in \mathbb{Z}. \quad (4–1)$$

[8] Note that for SO(odd) matrices there is always an eigenvalue at 1. The $N \to \infty$ scaling limit of the distribution of the second eigenangle for SO(odd) matrices equals the $N \to \infty$ scaling limit of the distribution of the first eigenangle for USp (unitary symplectic) matrices; see [Katz and Sarnak 99a pp. 10–11, 411–416] and [Katz and Sarnak 99b p. 10].

We often denote the curve by $[a_1, a_2, a_3, a_4, a_6]$. We let a_1 range from 0 to 10 (since without loss of generality we may assume $a_1 \geq 0$) and the other a_i range from -10 to 10. We kept only nonsingular curves. We took minimal Weierstrass models for the ones left, and pruned the list to ensure that all the remaining curves were distinct. We then analyzed the first few zeros above the central point for 1500 of these curves (due to the length of time it takes to compute zeros for the curves, it was impossible to analyze the entire set).

Figures 3 and 4 suggest that as the conductor increases, the repulsion decreases. For the larger conductors in Figure 4, the results are closer to the predictions of Katz–Sarnak, and the shape of the distribution with larger conductors is closer to the random-matrix theory plots of Figure 1. Though both plots in Figures 3 and 4 differ from the random-matrix-theory plots, the plot in Figure 4 is more peaked, the peak occurs earlier, and the decay in the tail is faster. Standard statistical tests show that the two means (1.04 for the smaller conductors and 0.88 for the larger) are significantly different. Two possible tests are the pooled two-sample t-procedure[9] (where we assume that the data are independently drawn from two normal distributions with the same mean and variance) and the unpooled two-sample t-procedure[10] (where we assume that the data are independently drawn from two normal distributions with the same mean and no assumption is made on the variance). See, for example, [Casella and Berger 02, pp. 409–410]. Both tests give t-statistics around 10.5 with over 1400 degrees of freedom. Since the number of degrees of freedom is so large, we may use the central limit theorem and replace the t-statistic with a z-statistic. Since for the standard normal the probability of being at least 10.5 standard deviations from zero is less than 3.2×10^{-12} percent, we obtain strong evidence against the null hypothesis that the two means are equal (i.e., we obtain evidence that the repulsion decreases as the conductor increases).

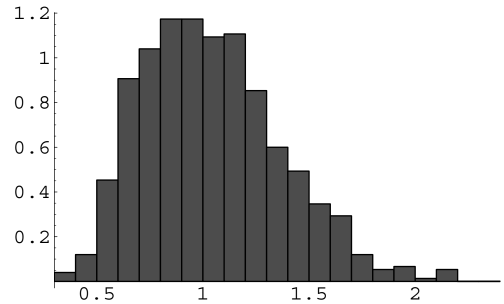

FIGURE 3. First normalized zero above the central point: 750 rank-0 curves from $y^2 + a_1xy + a_3y = x^3 + a_2x^2 + a_4x + a_6$, $\log(\text{cond}) \in [3.2, 12.6]$, median $= 1.00$, mean $= 1.04$, standard deviation about the mean $= .32$.

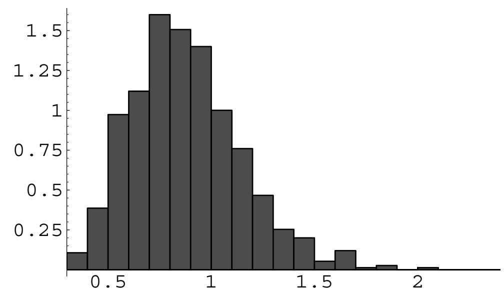

FIGURE 4. First normalized zero above the central point: 750 rank-0 curves from $y^2 + a_1xy + a_3y = x^3 + a_2x^2 + a_4x + a_6$, $\log(\text{cond}) \in [12.6, 14.9]$, median $= .85$, mean $= .88$, standard deviation about the mean $= .27$.

4.2.2 Rank-2 Curves. We study the first normalized zero above the central point for 1330 rank-2 elliptic curves, 665 with $\log(\text{cond}) \in [10, 10.3125]$ in Figure 5 and 665 with $\log(\text{cond}) \in [16, 16.5]$ in Figure 6. These curves were obtained from the same procedure that generated the 1500 curves in Section 4.2.1, except now we chose 1330 curves with what we believe is analytic rank exactly 2. We did this by showing that the L-function has even sign, the value at the central point is zero to at least five digits, and the second derivative at the central point is nonzero; see also Footnote 1. In Sections 4.3 Section 4.4 we study other families of curves of rank 2 (rank-2 curves from rank-0 and rank-2 one-parameter families over $\mathbb{Q}$).

[9]The pooled two-sample t-procedure is

$$t = (\overline{X_1} - \overline{X_2}) \Big/ s_p \sqrt{\frac{1}{n_1} + \frac{1}{n_2}},$$

where $\overline{X_i}$ is the sample mean of n_i observations of population i, s_i is the sample standard deviation, and

$$s_p = \sqrt{\frac{(n_1-1)s_1^2 + (n_2-1)s_2^2}{n_1+n_2-2}}$$

is the pooled variance; t has a t-distribution with $n_1 + n_2 - 2$ degrees of freedom.

[10]The unpooled two-sample t-procedure is

$$t = (\overline{X_1} - \overline{X_2}) \Big/ \sqrt{\frac{s_1^2}{n_1} + \frac{s_2^2}{n_2}};$$

this is approximately a t-distribution with

$$\frac{(n_1-1)(n_2-1)(n_2 s_1^2 + n_1 s_2^2)^2}{(n_2-1)n_2^2 s_1^4 + (n_1-1)n_1^2 s_2^4}$$

degrees of freedom.

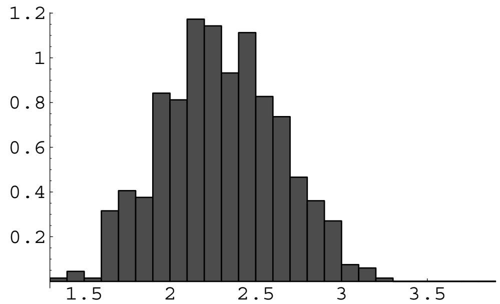

FIGURE 5. First normalized zero above the central point: 665 rank-2 curves from $y^2+a_1xy+a_3y = x^3+a_2x^2+a_4x+a_6$. $\log(\text{cond}) \in [10, 10.3125]$, median = 2.29, mean = 2.30.

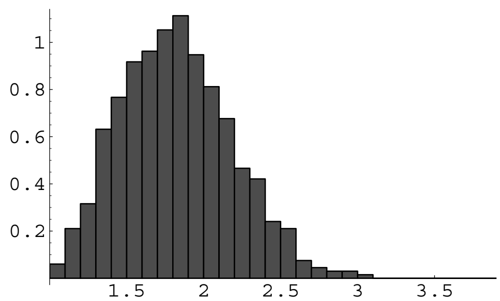

FIGURE 6. First normalized zero above the central point: 665 rank-2 curves from $y^2+a_1xy+a_3y = x^3+a_2x^2+a_4x+a_6$. $\log(\text{cond}) \in [16, 16.5]$, median = 1.81, mean = 1.82.

The results are very noticeable. The first normalized zero is significantly higher here than for the rank-0 curves. This supports the belief that for small conductors, the repulsion of the first normalized zero increases with the number of zeros at the central point.

We again split the data into two sets (Figures 5 and 6) based on the size of the conductor. As the conductors increase, the mean (and hence the repulsion) significantly decreases, from 2.30 to 1.82.

We are investigating rank-2 curves from the family of all elliptic curves (which is a many-parameter rank-0 family). In the limit we believe that half of the curves are of rank 0 and half are of rank 1. The natural question is to determine the appropriate model for this subset of curves. Since in the limit we believe that a curve has rank 2 (or more) with probability zero, this is a question about conditional probabilities.

4.3 One-Parameter Families of Rank 0 over the Rationals

4.3.1 Rank-0 Curves. We analyzed 14 one-parameter families of rank 0 over $\mathbb{Q}$; we chose these families from [Fermigier 96]. We want to study rank-0 curves in a solitary one-parameter family; however, the conductors grow rapidly and we can analyze only the first few zeros from a small number of curves in a family. For our conductor ranges it takes several hours of computer time to find the first few zeros for all the curves in a family. In Figures 7 and 8 and Tables 1 and 2 we study the first normalized zero above the central point for 14 one-parameter families of elliptic curves of rank 0 over $\mathbb{Q}$. Even though we have few data points in each family, we note that the medians and means are always higher for the smaller conductors than for the larger ones. Thus the "repulsion" is decreasing with increasing conductor, though perhaps repulsion is the wrong word here, since there is no zero at the central point! We studied the median as well as the mean, because for small data sets, one or two outliers can significantly affect the mean; the median is more robust.

For both the pooled and unpooled two-sample t-procedures the t-statistic exceeds 20 with over 200 degrees of freedom. The central limit theorem is an excellent approximation, yielding a z-statistic exceeding 20, which strongly argues for rejecting the null hypothesis that the two means are equal (i.e., providing evidence that the repulsion decreases with increasing conductors). Note that the first normalized zero above the central point is significantly larger than the $N \to \infty$ scaling limit of $\text{SO}(2N)$ matrices, which is about 0.321.

Some justification is required for regarding the data from the 14 families as independent samples from the same distribution. It is possible that there are family-specific lower-order terms to the n-level densities (see [Miller 02, Miller 05, Young 06]). Our amalgamation of the data is similar to what physicists do in combining the energy-level data from different heavy nuclei with similar quantum numbers. The hope is that the systems are similar enough to justify such averaging, since it is impractical to obtain sufficient data for just one nucleus (or one family of elliptic curves, as we see in Section 4.4). See also Remark 4.1.

Remark 4.2. The families are not independent: there are 11 curves that occur twice and one that occurs three times in the small-conductor set of 220 curves, and 133 repeats in the large-conductor set of 996 curves. In our amalgamations of the families, we present the results when we double count these curves as well as when we keep only one curve in each repeated set. In both cases the repeats account for a sizable percentage of the total number of observations; however, there is no significant difference between the two sets. Any curve can be placed in infinitely many one-parameter families; given polyno-

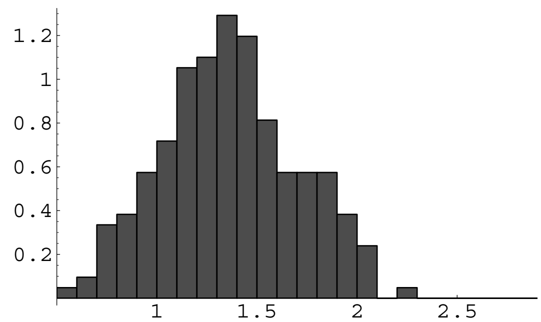

FIGURE 7. First normalized zero above the central point. 209 rank-0 curves from 14 rank-0 one-parameter families, $\log(\text{cond}) \in [3.26, 9.98]$, median = 1.35, mean = 1.36.

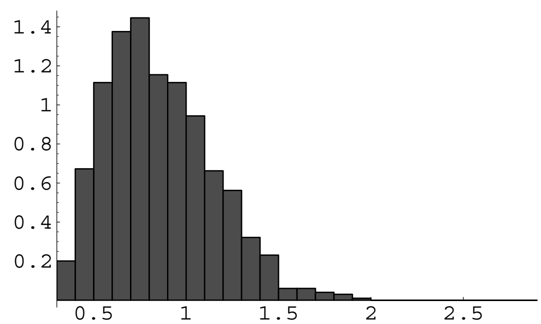

FIGURE 8. First normalized zero above the central point. 996 rank-0 curves from 14 rank 0 one-parameter families, $\log(\text{cond}) \in [15.00, 16.00]$, median = .81, mean = .86.

mials of sufficiently high degree we can force any number of curves to lie in two distinct families. Thus it is not surprising that we run into such problems when we amalgamate. When we remove the repeated curves, the pooled and unpooled two-sample t-procedures still give t-statistics exceeding 20 with over 200 degrees of freedom, indicating that the two means significantly differ and supporting the claim that the repulsion decreases with increasing conductor.

4.3.2 Rank-2 Curves. The previous results were for well-separated ranges of conductors. Since the first set often has very small log-conductors, it is possible that those values are anomalous. We therefore study two sets of curves for which the log-conductors, while different, are close in value. The goal is to see whether we can detect the effect of slight differences in the log-conductors on the repulsions.

Table 3 provides the data from an analysis of 21 rank-0 one-parameter families of elliptic curves over $\mathbb{Q}$. The families are from [Fermigier 96]. In each family, t ranges from -1000 to 1000. We searched for rank-2 curves with log-conductor in $[15, 16]$. Although we study rank-2 curves from families of rank 2 over $\mathbb{Q}$ in Section 4.4, there the conductors are so large that we can analyze only a few curves in each family. In particular, there are not enough curves in one family with conductors approximately equal to detect how slight differences in the log-conductors affect the repulsions.

We split these rank-2 curves from the 21 one-parameter families of rank 0 over $\mathbb{Q}$ into two sets: those curves with log-conductor in $[15, 15.5)$ and those with log-conductor in $[15.5, 16]$. We compared the two sets to see whether we could detect the decrease in repulsion for such small changes of the conductor. We have 21 families, with 350 curves in the small-conductor set and 388 in the large-conductor set.

Remark 4.3. The families are not independent: there are 15 curves that occur twice in the small-conductor set, and 22 in the larger. In our amalgamations of the families we consider both the case in which we do not remove these curves and the case in which we do. There is no significant difference in the results (the only noticeable change in the table is for the mean for the larger conductors, which increases from 1.9034 to 1.9052 and thus is rounded differently). See also Remark 4.2.

The medians and means of the small-conductor set are greater than those from the large-conductor set. For all curves the pooled and unpooled two-sample t-procedures give t-statistics of 2.5 with over 600 degrees of freedom; for distinct curves the pooled t-statistic is 2.16 (the unpooled t-statistic is 2.17) with over 600 degrees of freedom. Since the number of degrees of freedom is so large, we may use the central limit theorem. Since there is about a 3% chance of observing a z-statistic of 2.16 or greater, the results provide evidence against the null hypothesis (that the means are equal) at the .05 confidence level, though not at the .01 confidence level.

While the data suggest that the repulsion decreases with increasing conductor, it is not as clear as in our earlier investigations (where we had z-values greater than 10). This is, of course, due to the closeness of the two ranges of conductors. We apply nonparametric tests to further support our claim that the repulsion decreases with increasing conductors. For each family in Table 3, write a plus sign if the small-conductor set has a greater mean and a minus sign if not. There are four minus signs and seventeen plus signs. The null hypothesis is that each mean is equally likely to be larger. Under the null hy-

Family	Median $\widetilde{\mu}$	Mean μ	StDev σ_μ	log(conductor)	No.
1: $[0,1,1,1,T]$	1.28	1.33	0.26	$[3.93, 9.66]$	7
2: $[1,0,0,1,T]$	1.39	1.40	0.29	$[4.66, 9.94]$	11
3: $[1,0,0,2,T]$	1.40	1.41	0.33	$[5.37, 9.97]$	11
4: $[1,0,0,-1,T]$	1.50	1.42	0.37	$[4.70, 9.98]$	20
5: $[1,0,0,-2,T]$	1.40	1.48	0.32	$[4.95, 9.85]$	11
6: $[1,0,0,T,0]$	1.35	1.37	0.30	$[4.74, 9.97]$	44
7: $[1,0,1,-2,T]$	1.25	1.34	0.42	$[4.04, 9.46]$	10
8: $[1,0,2,1,T]$	1.40	1.41	0.33	$[5.37, 9.97]$	11
9: $[1,0,-1,1,T]$	1.39	1.32	0.25	$[7.45, 9.96]$	9
10: $[1,0,-2,1,T]$	1.34	1.34	0.42	$[3.26, 9.56]$	9
11: $[1,1,-2,1,T]$	1.21	1.19	0.41	$[5.73, 9.92]$	6
12: $[1,1,-3,1,T]$	1.32	1.32	0.32	$[5.04, 9.98]$	11
13: $[1,-2,0,T,0]$	1.31	1.29	0.37	$[4.73, 9.91]$	39
14: $[-1,1,-3,1,T]$	1.45	1.45	0.31	$[5.76, 9.92]$	10
All Curves	1.35	1.36	0.33	$[3.26, 9.98]$	209
Distinct Curves	1.35	1.36	0.33	$[3.26, 9.98]$	196

TABLE 1. First normalized zero above the central point for 14 one-parameter families of elliptic curves of rank 0 over $\mathbb{Q}$ (smaller conductors).

Family	Median $\widetilde{\mu}$	Mean μ	StDev σ_μ	log(conductor)	No.
1: $[0,1,1,1,T]$	0.80	0.86	0.23	$[15.02, 15.97]$	49
2: $[1,0,0,1,T]$	0.91	0.93	0.29	$[15.00, 15.99]$	58
3: $[1,0,0,2,T]$	0.90	0.94	0.30	$[15.00, 16.00]$	55
4: $[1,0,0,-1,T]$	0.80	0.90	0.29	$[15.02, 16.00]$	59
5: $[1,0,0,-2,T]$	0.75	0.77	0.25	$[15.04, 15.98]$	53
6: $[1,0,0,T,0]$	0.75	0.82	0.27	$[15.00, 16.00]$	130
7: $[1,0,1,-2,T]$	0.84	0.84	0.25	$[15.04, 15.99]$	63
8: $[1,0,2,1,T]$	0.90	0.94	0.30	$[15.00, 16.00]$	55
9: $[1,0,-1,1,T]$	0.86	0.89	0.27	$[15.02, 15.98]$	57
10: $[1,0,-2,1,T]$	0.86	0.91	0.30	$[15.03, 15.97]$	59
11: $[1,1,-2,1,T]$	0.73	0.79	0.27	$[15.00, 16.00]$	124
12: $[1,1,-3,1,T]$	0.98	0.99	0.36	$[15.01, 16.00]$	66
13: $[1,-2,0,T,0]$	0.72	0.76	0.27	$[15.00, 16.00]$	120
14: $[-1,1,-3,1,T]$	0.90	0.91	0.24	$[15.00, 15.99]$	48
All Curves	0.81	0.86	0.29	$[15.00, 16.00]$	996
Distinct Curves	0.81	0.86	0.28	$[15.00, 16.00]$	863

TABLE 2. First normalized zero above the central point for 14 one-parameter families of elliptic curves of rank 0 over $\mathbb{Q}$ (larger conductors).

pothesis, the number of minus signs is a random variable from a binomial distribution with $N = 21$ and $\theta = \frac{1}{2}$. The probability of observing four or fewer minus signs is about 3.6%, supporting the claim of decreasing repulsion with increasing conductor. For the medians there are seven minus signs out of twenty-one; the probability of seven or fewer minus signs is about 9.4%. Every time the smaller-conductor set had the lesser mean, it also had the lesser median; the mean and median tests are not independent.

4.4 One-Parameter Families of Rank 2 over the Rationals

4.4.1 The Family $y^2 = x^3 - T^2x + T^2$. We study the first normalized zero above the central point for 69 rank-2 elliptic curves from the one-parameter family $y^2 = x^3 - T^2x + T^2$ of rank 2 over $\mathbb{Q}$. There are 35 curves with $\log(\text{cond}) \in [7.8, 16.1]$ in Figure 9 and 34 with $\log(\text{cond}) \in [16.2, 23.3]$ in Figure 10. Unlike the previous examples in which we chose many curves of the same rank from different families, here we have just one family. Since the conductors grow rapidly, we have far fewer data points, and the range of the log-conductors is much greater. However, even for such a small sample, the repulsion decreases with increasing conductors, and the shape begins to approach the conjectured distribution. The pooled and unpooled two-sample t-procedures give t-statistics over 5 with over 60 degrees of freedom, and we may use the central limit theorem. Since the probability of a z-value of 5 or more is less than $10^{-4}\%$, the data do not support the null hypothesis (i.e., the data support our conjecture that the repulsion decreases as the conductors increase).

4.4.2 Rank-2 Curves. We consider 21 one-parameter families of rank 2 over $\mathbb{Q}$, and investigate curves of rank 2 in these families. The families are from [Fermigier 96]. We again amalgamated the different families, and summarize the results in Table 4.

The difference between these experiments and those of Section 4.3.2 is that while both deal with one-parameter families over $\mathbb{Q}$, here we study curves of rank 2 from families of rank 2 over $\mathbb{Q}$; earlier we studied curves of rank

Family	$\widetilde{\mu}$	μ	σ_μ	No.	$\widetilde{\mu}$	μ	σ_μ	No.
1: $[0,1,3,1,T]$	1.59	1.83	0.49	8	1.71	1.81	0.40	19
2: $[1,0,0,1,T]$	1.84	1.99	0.44	11	1.81	1.83	0.43	14
3: $[1,0,0,2,T]$	2.05	2.03	0.26	16	2.08	1.94	0.48	19
4: $[1,0,0,-1,T]$	2.02	1.98	0.47	13	1.87	1.94	0.32	10
5: $[1,0,0,T,0]$	2.05	2.02	0.31	23	1.85	1.99	0.46	23
6: $[1,0,1,1,T]$	1.74	1.85	0.37	15	1.69	1.77	0.38	23
7: $[1,0,1,2,T]$	1.92	1.95	0.37	16	1.82	1.81	0.33	14
8: $[1,0,1,-1,T]$	1.86	1.88	0.34	15	1.79	1.87	0.39	22
9: $[1,0,1,-2,T]$	1.74	1.74	0.43	14	1.82	1.90	0.40	14
10: $[1,0,-1,1,T]$	2.00	2.00	0.32	22	1.81	1.94	0.42	18
11: $[1,0,-2,1,T]$	1.97	1.99	0.39	14	2.17	2.14	0.40	18
12: $[1,0,-3,1,T]$	1.86	1.88	0.34	15	1.79	1.87	0.39	22
13: $[1,1,0,T,0]$	1.89	1.88	0.31	20	1.82	1.88	0.39	26
14: $[1,1,1,1,T]$	2.31	2.21	0.41	16	1.75	1.86	0.44	15
15: $[1,1,-1,1,T]$	2.02	2.01	0.30	11	1.87	1.91	0.32	19
16: $[1,1,-2,1,T]$	1.95	1.91	0.33	26	1.98	1.97	0.26	18
17: $[1,1,-3,1,T]$	1.79	1.78	0.25	13	2.00	2.06	0.44	16
18: $[1,-2,0,T,0]$	1.97	2.05	0.33	24	1.91	1.92	0.44	24
19: $[-1,1,0,1,T]$	2.11	2.12	0.40	21	1.71	1.88	0.43	17
20: $[-1,1,-2,1,T]$	1.86	1.92	0.28	23	1.95	1.90	0.36	18
21: $[-1,1,-3,1,T]$	2.07	2.12	0.57	14	1.81	1.81	0.41	19
All Curves	1.95	1.97	0.37	350	1.85	1.90	0.40	388
Distinct Curves	1.95	1.97	0.37	335	1.85	1.91	0.40	366

TABLE 3. First normalized zero above the central point for rank-2 curves from one-parameter families of rank 0 over $\mathbb{Q}$. The first set are curves with $\log(\text{cond}) \in [15, 15.5)$; the second set are curves with $\log(\text{cond}) \in [15.5, 16]$. Median $= \widetilde{\mu}$, mean $= \mu$, standard deviation (about the mean) $= \sigma_\mu$.

2 from families of rank 0 over $\mathbb{Q}$. If the density conjecture (with orthogonal groups) is correct for the entire one-parameter family, in the limit 0% of the curves in a family of rank r have rank $r+2$ or greater. Thus our previous investigations of curves of rank 2 in a family of rank 0 over $\mathbb{Q}$ were a study of a measure-zero subset. Unlike curves of rank 2 in families of rank 2 over $\mathbb{Q}$, we have no theoretical evidence supporting a proposed random-matrix model for curves of rank 2 in families of rank 0. We compare the results from rank-2 curves in rank-2 families over $\mathbb{Q}$ to the rank-2 curves from rank-0 families over $\mathbb{Q}$ in Section 4.5.

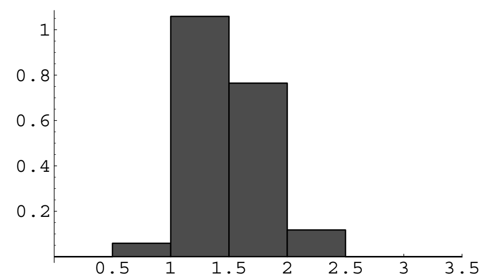

FIGURE 10. First normalized zero above the central point from rank-2 curves in the family $y^2 = x^3 - T^2x + T^2$; 34 curves, $\log(\text{cond}) \in [16.2, 23.3]$, median $= 1.37$, mean $= 1.47$, standard deviation about the mean $= .34$.

Remark 4.4. There are 23 rank-4 curves in the 21 one-parameter families of rank 2 over $\mathbb{Q}$ with log-conductors in $[15, 16]$ and $t \in [0, 120]$. For the first normalized zero above the central point, the median is 3.03, the mean is 3.05, and the standard deviation about the mean is 0.30.

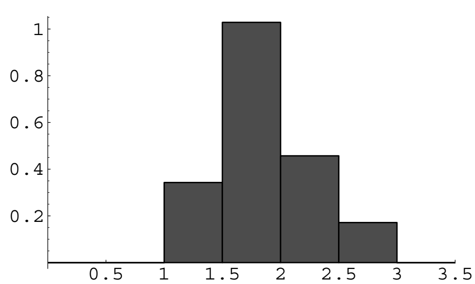

FIGURE 9. First normalized zero above the central point from rank-2 curves in the family $y^2 = x^3 - T^2x + T^2$; 35 curves, $\log(\text{cond}) \in [7.8, 16.1]$, median $= 1.85$, mean $= 1.92$, standard deviation about the mean $= .41$.

4.5 Comparison between One-Parameter Families of Different Ranks

In Table 5 we investigate how the first normalized zero above the central point of rank-2 curves depends on how the curves are obtained. The first family is rank-2 curves from the 21 one-parameter families of rank 0 over $\mathbb{Q}$ from Table 3, while the second is rank-2 curves from the 21 one-parameter families of rank 2 over $\mathbb{Q}$ from Table 4; in both sets the log-conductors are in $[15, 16]$. A t-test on the two means gives a t-statistic of 6.60, indicating that the two means differ. Thus the mean of the first normalized zero above the central point of rank-2 curves in a one-parameter family over $\mathbb{Q}$ (for conductors in this

Family	Mean	Standard Deviation	log(conductor)	No.
1: $[1, T, 0, -3-2T, 1]$	1.91	0.25	$[15.74, 16.00]$	2
2: $[1, T, -19, -T-1, 0]$	1.57	0.36	$[15.17, 15.63]$	4
3: $[1, T, 2, -T-1, 0]$	1.29		$[15.47, 15.47]$	1
4: $[1, T, -16, -T-1, 0]$	1.75	0.19	$[15.07, 15.86]$	4
5: $[1, T, 13, -T-1, 0]$	1.53	0.25	$[15.08, 15.91]$	3
6: $[1, T, -14, -T-1, 0]$	1.69	0.32	$[15.06, 15.22]$	3
7: $[1, T, 10, -T-1, 0]$	1.62	0.28	$[15.70, 15.89]$	3
8: $[0, T, 11, -T-1, 0]$	1.98		$[15.87, 15.87]$	1
9: $[1, T, -11, -T-1, 0]$				
10: $[0, T, 7, -T-1, 0]$	1.54	0.17	$[15.08, 15.90]$	7
11: $[1, T, -8, -T-1, 0]$	1.58	0.18	$[15.23, 25.95]$	6
12: $[1, T, 19, -T-1, 0]$				
13: $[0, T, 3, -T-1, 0]$	1.96	0.25	$[15.23, 15.66]$	3
14: $[0, T, 19, -T-1, 0]$				
15: $[1, T, 17, -T-1, 0]$	1.64	0.23	$[15.09, 15.98]$	4
16: $[0, T, 9, -T-1, 0]$	1.59	0.29	$[15.01, 15.85]$	5
17: $[0, T, 1, -T-1, 0]$	1.51		$[15.99, 15.99]$	1
18: $[1, T, -7, -T-1, 0]$	1.45	0.23	$[15.14, 15.43]$	4
19: $[1, T, 8, -T-1, 0]$	1.53	0.24	$[15.02, 15.89]$	10
20: $[1, T, -2, -T-1, 0]$	1.60		$[15.98, 15.98]$	1
21: $[0, T, 13, -T-1, 0]$	1.67	0.01	$[15.01, 15.92]$	2
All Curves	1.61	0.25	$[15.01, 16.00]$	64

TABLE 4. First normalized zero above the central point for 21 one-parameter families of rank 2 over $\mathbb{Q}$ with $\log(\text{cond}) \in [15, 16]$ and $t \in [0, 120]$. The median of the first normalized zero of the 64 curves is 1.64.

Curves / Family	Median	Mean	Std. Dev.	No.
Rank 2 / Rank 0 over $\mathbb{Q}$	1.926	1.936	0.388	701
Rank 2 / Rank 2 over $\mathbb{Q}$	1.642	1.610	0.247	64

TABLE 5. First normalized zero above the central point. The first family is the 7014 rank-2 curves from the 21 one-parameter families of rank 0 over $\mathbb{Q}$ from Table 3 with $\log(\text{cond}) \in [15, 16]$; the second family is the 64 rank-2 curves from the 21 one-parameter families of rank 2 over $\mathbb{Q}$ from Table 4 with $\log(\text{cond}) \in [15, 16]$.

	863 Rank-0 Curves	701 Rank-2 Curves	t-Statistic
Median $z_2 - z_1$	1.28	1.30	
Mean $z_2 - z_1$	1.30	1.34	-1.60
StDev $z_2 - z_1$	0.49	0.51	
Median $z_3 - z_2$	1.22	1.19	
Mean $z_3 - z_2$	1.24	1.22	0.80
StDev $z_3 - z_2$	0.52	0.47	
Median $z_3 - z_1$	2.54	2.56	
Mean $z_3 - z_1$	2.55	2.56	-0.38
StDev $z_3 - z_1$	0.52	0.52	

TABLE 6. Spacings between normalized zeros. All curves have $\log(\text{cond}) \in [15, 16]$, and z_j is the imaginary part of the jth normalized zero above the central point. The 863 rank-0 curves are from the 14 one-parameter families of rank 0 over $\mathbb{Q}$ from Table 2; the 701 rank-2 curves are from the 21 one-parameter families of rank 0 over $\mathbb{Q}$ from Table 3.

range) depends on *how* we choose the curves. For the range of conductors studied, rank-2 curves from rank-0 one-parameter families over $\mathbb{Q}$ do *not* behave the same as rank-2 curves from rank-2 one-parameter families over $\mathbb{Q}$.

4.6 Spacings between Normalized Zeros

For finite conductors, even when there are no zeros at the central point, the first normalized zero above the central point is repelled from the predicted $N \to \infty$ scaling limits. The repulsion increases with the number of zeros at the central point and decreases with increasing conductor. For an elliptic curve E, let $z_1, z_2, z_3, \ldots$ denote the imaginary parts of the normalized zeros above the central point. We investigate whether $z_{j+1} - z_j$ depends on the repulsion from the central point.

We consider the following two sets of curves in Table 6:

- the 863 distinct rank-0 curves with $\log(\text{cond}) \in [15, 16]$ from the 14 one-parameter families of rank 0 over $\mathbb{Q}$ from Table 2;
- the 701 distinct rank-2 curves with $\log(\text{cond}) \in [15, 16]$ from the 21 one-parameter families of rank 0 over $\mathbb{Q}$ from Table 3.

In Table 6 we calculate the median and mean for $z_2 - z_1$, $z_3 - z_2$, and $z_3 - z_1$. The last statistic involves the sum of differences between two adjacent normalized zeros, and allows the possibility of some effects being averaged out. Although the normalized zeros are repelled from the central point (and by different amounts for the two sets), the *differences* between the normalized zeros are statistically independent of this repulsion. We performed a t-test on the means in the three cases. In each case, the t-statistic was less than 2, strongly supporting the null hypothesis that the differences are independent of the repulsion.

We have consistently observed that the greater the number of zeros at the central point, the greater the repulsion. One possible explanation is as follows: For rank-2 curves in a rank-0 one-parameter family over $\mathbb{Q}$, the first zero above the central point collapses down to the central point, and the other zeros are left alone. Since the zeros are symmetric about the central point, the effect of one zero above the central point collapsing is to increase the number of zeros at the central point by 2.

For our 14 one-parameter families of elliptic curves of rank 0 over $\mathbb{Q}$ and log-conductors in $[15, 16]$, we studied the second and third normalized zeros above the central point. The mean of the second normalized zero is 2.16 with a standard deviation of .39, while the third normalized zero has a mean of 3.41 and a standard deviation of .41. These numbers differ statistically[11] from the first and second normalized zeros of the rank-2 curves from our 21 one-parameter families of rank 0 over $\mathbb{Q}$ with log-conductor in $[15, 16]$, where the means were respectively 1.93 (with a standard deviation of .39) and 3.27 (with a standard deviation of .39). Thus while for a given range of log-conductors the average second normalized zero of a rank-0 curve is close to the average first normalized zero of a rank-2 curve, they are not equal, and the additional repulsion from extra zeros at the central point cannot be entirely explained *only* by collapsing the first zero to the central point while leaving the other zeros alone.

Remark 4.5. Since the second (respectively third) normalized zero for rank-0 curves in rank-0 families over $\mathbb{Q}$ is 2.16 (3.41) while the first (second) normalized zero for rank-2 curves in rank-0 families over $\mathbb{Q}$ is 1.93 (3.27), one can interpret the effect of the additional zeros at the central point as an *attraction*. Specifically, for curves of rank 2 in a rank-0 family over $\mathbb{Q}$, by symmetry, two zeros collapse to the central point, and the remaining zeros are then attracted to the central point, being closer than the corresponding zeros from rank-0 curves. As remarked in [Farmer 05, Section 3.5], the term "lowest zero" is not well defined when there are multiple zeros at the central point. We can mean either the first zero above the central point, or one of the many zeros at the central point. In all cases, for finite conductors there is repulsion from the $N \to \infty$ scaling limits of random-matrix theory; however, "attraction" might be a better term for the effect of additional zeros at the central point, though the current terminology is to talk about repulsion of zeros at the central point.

We now study the differences between normalized zeros coming from one-parameter families of rank 2 over $\mathbb{Q}$. Table 7 shows that while the normalized zeros are repelled from the central point, the *differences* between the normalized zeros are statistically independent of the repulsion. We performed a t-test for the means in the three cases studied. For two of the three cases the t-statistic was less than 2 (and in the third it was only 2.05), supporting the null hypothesis that the differences are independent of the repulsion.

[11] The pooled and unpooled t-statistics in both experiments are greater than 6, providing evidence against the null hypothesis that the two means are equal.

	64 Rank-2 Curves	23 Rank-4 Curves	t-Statistic
Median $z_2 - z_1$	1.26	1.27	
Mean $z_2 - z_1$	1.36	1.29	0.59
StDev $z_2 - z_1$	0.50	0.42	
Median $z_3 - z_2$	1.22	1.08	
Mean $z_3 - z_2$	1.29	1.14	1.35
StDev $z_3 - z_2$	0.49	0.35	
Median $z_3 - z_1$	2.66	2.46	
Mean $z_3 - z_1$	2.65	2.43	2.05
StDev $z_3 - z_1$	0.44	0.42	

TABLE 7. Spacings between normalized zeros. All curves have $\log(\text{cond}) \in [15, 16]$, and z_j is the imaginary part of the jth normalized zero above the central point. The 64 rank-2 curves are the 21 one-parameter families of rank 2 over $\mathbb{Q}$ from Table 4; the 23 rank-4 curves are the 21 one-parameter families of rank 2 over $\mathbb{Q}$ from Table 4.

	701 Rank-2 Curves	64 Rank-2 Curves	t-Statistic
Median $z_2 - z_1$	1.30	1.26	
Mean $z_2 - z_1$	1.34	1.36	0.69
StDev $z_2 - z_1$	0.51	0.50	
Median $z_3 - z_2$	1.19	1.22	
Mean $z_3 - z_2$	1.22	1.29	1.39
StDev $z_3 - z_2$	0.47	0.49	
Median $z_3 - z_1$	2.56	2.66	
Mean $z_3 - z_1$	2.56	2.65	1.93
StDev $z_3 - z_1$	0.52	0.44	

TABLE 8. Spacings between normalized zeros. All curves have $\log(\text{cond}) \in [15, 16]$, and z_j is the imaginary part of the jth normalized zero above the central point. The 701 rank-2 curves are the 21 one-parameter families of rank 0 over $\mathbb{Q}$ from Table 4, and the 64 rank-2 curves are the 21 one-parameter families of rank 2 over $\mathbb{Q}$ from Table 4.

We performed one last experiment on the differences between normalized zeros. In Table 8 we compare two sets of rank-2 curves: the first are the 21 one-parameter families of rank 0 over $\mathbb{Q}$ from Table 3, while the second are the 21 one-parameter families of rank 2 over $\mathbb{Q}$ from Table 4. While the first normalized zero is repelled differently in the two cases, the differences are statistically independent of the nature of the zeros at the central point, as indicated by all t-statistics being less than 2. This suggests that the *spacings* between adjacent normalized zeros above the central point are independent of the repulsion at the central point; in particular, this quantity does not depend on how we construct our family of rank-2 curves.

5. SUMMARY AND FUTURE WORK

As the conductors tend to infinity, theoretical results support the validity of the $N \to \infty$ scaling limit of the independent model for all curves in one-parameter families of elliptic curves of rank r over $\mathbb{Q}$; however, it is unknown what the correct model is for the subfamily of curves of rank $r+2$. The experimental evidence suggests that the first normalized zero, for small and finite conductors, is repelled by zeros at the central point. Further, the greater the number of zeros at the central point, the greater the repulsion; however, the repulsion decreases as the conductors increase, and the difference between adjacent normalized zeros is statistically independent of the repulsion and the rank of the curves.

At present, we can calculate the first normalized zero for log-conductors of size about 25. While we can use more powerful computers to study larger conductors, it is unlikely that these conductors will be large enough to exhibit the predicted limiting behavior. It is interesting that in contrast to the excess-rank investigations, here we see noticeable convergence to the limiting theoretical results as we increase the conductors.

An interesting project is to determine a theoretical model to explain the behavior for finite conductors. In the large-conductor limit, analogies with the function field and calculations with the explicit formula lead us to the independent model for curves of rank r from families of rank r over $\mathbb{Q}$, and theoretical results in the number-field case support this. It is not unreasonable to posit that in the finite-conductor analogues the size of the matrices should be a function of the log-conductors. Unfortunately, the statistics for the finite $N \times N$ random-matrix ensembles are expressed in terms of eigenvalues of integral equations, and are usually plotted only in the $N \to \infty$ scaling limit. This makes comparison with the experimental data difficult, and a future project is to analyze the finite-N cases using the finite-N kernels. Such an analysis will facilitate comparing the finite-N limits of the independent and interaction models for curves of rank $r+2$ from families of rank r over $\mathbb{Q}$.

APPENDIX A. "HARDER" ENSEMBLES OF ORTHOGONAL MATRICES

(written by Eduardo Dueñez)

In this appendix we derive the conditional (interaction) eigenvalue probability measure (2–4) and illustrate how it affects eigenvalue statistics near the central point 1, in particular through repulsion (observed via the 1-level density). We also explain the relation to the classical Bessel kernels of random-matrix theory, and to other central-point statistics.

A.1 Full Orthogonal Ensembles

In view of our intended application, we will be concerned exclusively with random-matrix ensembles of orthogonal matrices in what follows. If we write the eigenvalues (in no particular order) of a special[12] orthogonal matrix of size $2N$ (respectively $2N+1$) as $\{\pm e^{i\theta_j}\}_1^N$ (respectively $\{+1\} \cup \{\pm e^{i\theta_j}\}_1^N$) with $0 \le \theta_j \le \pi$, then the N-tuple $\Theta = (\theta_1, \dots, \theta_N)$ parameterizes the eigenvalues. In terms of the angles θ_j, the probability measure of the eigenvalues induced from normalized Haar measure on $\mathrm{SO}(2N)$ (respectively on $\mathrm{SO}(2N+1)$ upon discarding one forced eigenvalue of $+1$) can be identified with a measure on $[0, \pi]^N$,

$$d\varepsilon_0(\Theta) = \tilde{C}_N^{(0)} \prod_{1 \le j < k \le N} (\cos\theta_k - \cos\theta_j)^2 \prod_{1 \le j \le N} d\theta_j, \tag{A–1}$$

$$d\varepsilon_1(\Theta) = \tilde{C}_N^{(1)} \prod_{1 \le j < k \le N} (\cos\theta_k - \cos\theta_j)^2 \times \prod_{1 \le j \le N} \sin^2\left(\frac{\theta_j}{2}\right) d\theta_j \tag{A–2}$$

in the $2N$ and $2N+1$ cases, respectively, as shown in [Conrey 05, Katz and Sarnak 99a]; the normalization constants $\tilde{C}_N^{(m)}$ ensure that the measures on the right-hand sides are probability measures. Note that formulas (A–1) and (A–2) are symmetric upon permuting the θ_j's, so issues related to a choice of a particular ordering of the eigenvalues of the matrix are irrelevant. More importantly, observe the quadratic exponent of the differences of the cosines.

The statistical behavior of the eigenvalues near $+1$ is closely related to the order of vanishing of the measures above at $\theta = 0$. We change variables and replace the eigenvalues $e^{\pm i\theta}$ by the levels

$$x = \cos\theta \tag{A–3}$$

[12] That is, of determinant one.

so the measures above become measures on $[-1,+1]^N$:

$$d\varepsilon_0(X) = C_N^{(0)} \prod_{1\le j<k\le N} (x_k - x_j)^2 \times \prod_{j=1}^{N} (1-x_j)^{-1/2}(1+x_j)^{-1/2} dx_j, \qquad \text{(A–4)}$$

$$d\varepsilon_1(X) = C_N^{(1)} \prod_{j<k} (x_k - x_j)^2 \times \prod_{j=1}^{N} (1-x_j)^{1/2}(1+x_j)^{-1/2} dx_j, \qquad \text{(A–5)}$$

where $X = (x_1, \ldots, x_N)$ and $C_N^{(m)}$ are suitable normalization constants. Here we observe the appearance of the weight functions on $[-1,1]$:

$$w(x) = (1-x)^a (1+x)^{-1/2}, \qquad \text{(A–6)}$$

$$a = \begin{cases} -\frac{1}{2} & \text{for } SO(2N), \\ +\frac{1}{2} & \text{for } SO(2N+1). \end{cases} \qquad \text{(A–7)}$$

By the Gaudin–Mehta theory (see, for example, [Mehta 91]), and in view of the quadratic exponent of the differences of the "levels" x_j, the study of eigenvalue statistics using classical methods is intimately related to the sequence of orthogonal polynomials with respect to the weight $w(x)$.[13]

In classical random-matrix-theory terminology (especially in the context of the Laguerre and Jacobi ensembles) the endpoints $-1, +1$ are called the "hard edges" of the spectrum because the probability measure, considered on $\mathbb{R}^N$, vanishes outside $[-1,+1]^N$. We will keep calling $\theta = 0$, π the "central points" (endpoints of the diameter with respect to which the spectrum is symmetric). Phenomena about central points and hard edges are equivalent in view of the change of variables (A–3). Perhaps not surprisingly, the parameter a, which dictates the order of vanishing of the weight function $w(x)$ at the hard edge $+1$, suffices to characterize the mutually different statistics near the central point in each of SO(even) and SO(odd). However, the importance of this parameter is best understood in the context of certain subensembles of SO as described below.

A.2 Conditional ("Harder") Orthogonal Ensembles

The conditional eigenvalue measure for the subensemble $SO^{(2r)}(2N)$ of $SO(2N)$ consisting of matrices for which some $2r$ of the $2N$ eigenvalues are equal to $+1$ can easily be obtained from (A–4). Let

$$f(x_1, \ldots, x_N) = C_N^{(m)} \prod_{1\le j<k\le N} (x_k - x_j)^2 \prod_{1\le j\le N} w(x_j) \qquad \text{(A–8)}$$

be the normalized probability density function of the levels for $SO(2N)$, where $w(x)$ is as in (A–6) with $a = -\frac{1}{2}$ and $m = 0$. Now let $t_1, \ldots, t_r$ be chosen such that $0 < t_k < 1$, let $K = \prod_j [1-t_j, 1]$, and let $I = J \times K$ for some box $J \subset [-1,1]^{N-r}$. This means that we are constraining r pairs of levels to lie in a neighborhood of $x = 1$ (or equivalently that we are construing r pairs of eigenvalues to lie in circular sectors about the point 1 on the unit circle). Thus, the conditional probability that the remaining $N - r$ pairs of eigenvalues lie in J is given by

$$F(T; J) = \frac{\displaystyle\int_{J\times K} f(x)\,dx}{\displaystyle\int_{[-1,1]^{N-r}\times K} f(x)\,dx}, \qquad \text{(A–9)}$$

where $T = (t_1, \ldots, t_r)$. The conditional probability measure of the eigenvalues for the subensemble $SO^{(2r)}(2N)$ is the limit as all $t_k \to 0+$ of $F(t; J)$, as a function of the box J; call it $G(J)$. Applying L'Hôpital's rule r times to the quotient (A–9) (once on each variable t_k) and using the fundamental theorem of calculus we get

$$G(J) = \lim_{T\to 0+} \frac{\int_J (V(X))^2 (M(X,T))^2 w(X) dX \cdot (V(T))^2 w(T)}{\int_{[0,1]^{N-r}} (V(X))^2 (M(X,T))^2 w(X) dX \cdot (V(T))^2 w(T)}, \qquad \text{(A–10)}$$

where $X = (x_1, \ldots, x_{N-r})$ and

$$V(X) = \prod_{1\le j<k\le N-r} (x_k - x_j),$$

$$V(T) = \prod_{1\le j<k\le r} (t_k - t_j),$$

$$w(X) = \prod_{1\le j\le N-r} w(x_j),$$

$$w(T) = \prod_{1\le k\le r} w(1-t_k),$$

$$M(X,T) = \prod_{\substack{1\le j\le N-r \\ 1\le k\le r}} (1 - t_k - x_j).$$

Naturally, the factors of $V(T)$ and $w(T)$ cancel in equation (A–10). Since $M(X,T)$ is bounded, the integrands in equation (A–10) are uniformly dominated by an integrable function, ensuring that we can let all $t_j \to 0$ in the integrands of (A–10) to obtain

$$G(J) = \frac{\int_J (V(X))^2 (M(X,0))^2 w(X)\,dX}{\int_{[0,1]^{N-r}} (V(X))^2 (M(X,0))^2 w(X)\,dX}. \qquad \text{(A–11)}$$

[13] The inner product being $\langle f, g\rangle = \int_0^1 f(x)\overline{g(x)} w(x)\,dx$.

Now observe that $(M(X,0))^2 w(X) = \prod_{1\le j\le r} \widetilde{w}(x_j)$, where $\widetilde{w}(x)$ is given by equation (A–6) with a replaced by $\tilde{a} = a+2$, so the probability measure of the eigenvalues for $\mathrm{SO}^{(2r)}(2N)$ is obtained from that of $\mathrm{SO}(2(N-m))$ simply by changing the weight function $w \mapsto \widetilde{w}$. Explicitly, the probability measure of the eigenvalues of the ensemble $\mathrm{SO}^{(2r)}(2N)$ is given by

$$d\varepsilon_m(X) = C_{N-m}^{(m)} \prod_{j<k} (x_k - x_j)^2 \prod_j (1-x_j)^{m-1/2} \prod_j dx_j, \tag{A–12}$$

where $m = 2r$, $X = (x_1, \dots, x_{N-r})$, the indices j, k range from 1 to $N-r$, and $C_{N-m}^{(m)}$ are suitable normalization constants (equal to the reciprocal of the denominator of the right-hand side of equation (A–11)).

The same argument shows that the subensemble $\mathrm{SO}^{(2r+1)}(2N+1)$ of $\mathrm{SO}(2N+1)$ consisting of matrices for which $2r+1$ eigenvalues are equal to $+1$ has the same eigenvalue measure (A–12) with $m = 2r+1$. Because the density of the measure vanishes to a higher order near the edge $+1$ the larger m is, we will say that the edge becomes *harder* when m is larger (whence the title of this section), and call m its *hardness*.

A.3 Independent Model

It is important to observe that the presence of the m-multiple eigenvalues at the central point in these harder subensembles of orthogonal matrices has a strong repelling effect due to the extra factor $(1-x)^m$ multiplied by the weight $(1-x)^{-1/2}(1+x)^{-1/2}$ of SO(even). For comparison purposes consider the following situation, first in the SO(even) case. The number of eigenvalues equal to $+1$ of any $\mathrm{SO}(2N)$ matrix is always an even number $2r$, and one may consider the subensemble $\mathcal{A}_{2N,2r}$ of $\mathrm{SO}(2N)$,

$$\mathcal{A}_{2N,2r} = \left\{ \begin{pmatrix} I_{2r\times 2r} & \\ & g \end{pmatrix} : g \in \mathrm{SO}(2N-2r) \right\}, \tag{A–13}$$

which is just $\mathrm{SO}(2N-2r)$ in disguise. This is certainly a subensemble of $\mathrm{SO}(2N)$ consisting of matrices with at least $2r$ eigenvalues equal to $+1$, albeit quite a different one from the $2r$-hard subensemble of $\mathrm{SO}(2N)$ described before. For example, the eigenvalue measure (apart from the point masses at the last $2r$ eigenvalues) for $\mathcal{A}_{2N,2r}$ is

$$d\varepsilon_0(x_1, \dots, x_{N-r}), \tag{A–14}$$

and not $d\varepsilon_{2r}(x_1, \dots, x_{N-r})$. The same observation applies in the $\mathrm{SO}(2N+1)$ case: with the obvious notation, the eigenvalue measure for $\mathcal{A}_{2N+1,2r}$ is[14]

$$d\varepsilon_1(\theta_1, \dots, \theta_{N-r}), \tag{A–15}$$

and not $d\varepsilon_{2r+1}(\theta_1, \dots, \theta_{N-r})$.

A.4 1-Level Density: Full Orthogonal

Before dealing with the harder subensembles, we make some comments about the hard edges of the full SO(even) and SO(odd). The local statistics near the point $+1$ are dictated by the even "+" (respectively odd "−") sine kernels

$$S_\pm(\xi, \eta) = S(\xi, \eta) \pm S(\xi, -\eta) \tag{A–16}$$

in the case of SO(even) (respectively SO(odd)); see [Katz and Sarnak 99a, Katz and Sarnak 99b]. Here ξ, η are rescaled variables centered at the value 0, namely related to the original variables by[15]

$$x = \cos\left(\frac{\pi}{N}\xi\right), \tag{A–17}$$

and $S(x,y) = \sin(\pi x)/(\pi x)$ is the sine kernel, which has the universal property of describing the local statistics at *any* bulk point of *any* ensemble with local quadratic local level repulsion [Deift et al. 99]. However, it is not the sine kernel but its even (odd) counterparts that dictate the local statistics near the central point. For example, the central one-level density is given by the diagonal values at $x = y$ of the respective kernel (see Figure 11):

$$\rho_+(x) = 1 + \frac{\sin 2\pi x}{2\pi x}, \quad \text{for SO(even)}, \tag{A–18}$$

$$\rho_-(x) = 1 + \frac{\sin 2\pi x}{2\pi x} + \delta(x), \quad \text{for SO(odd)}. \tag{A–19}$$

(In the SO(odd) case the Dirac delta reflects the fact that any such matrix has an eigenvalue at the central point.) Observe that ρ_- vanishes to second order, whereas ρ_+ does not vanish at the central point $x = 0$.[16]

A.5 1-Level Density: Harder Orthogonal

We return to the more general case of m-hard ensembles of orthogonal matrices. Because the classical Jacobi polynomials $\left\{P_n^{(a,b)}\right\}_0^\infty$ are orthogonal with respect

[14] Observe that a matrix in $\mathcal{A}_{2N+1,2r}$ has $2r+1$ eigenvalues equal to $+1$ and $N-r$ other pairs of eigenvalues.

[15] This is justified by the fact N/π is the average (angular) *asymptotic* density of the eigenangles θ_j of a random orthogonal matrix; hence asymptotic equidistribution holds—away from the central points!

[16] If the central point were not atypical, then the local density would be dictated by the diagonal values $S(x,x) \equiv 1$ of the sine kernel.

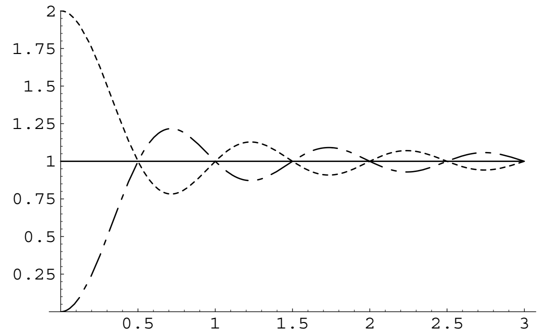

FIGURE 11. The central 1-level densities ρ_+ (dotted) and ρ_- (dash-dotted) versus the "bulk" 1-level density $\rho \equiv 1$ observed away from the central points.

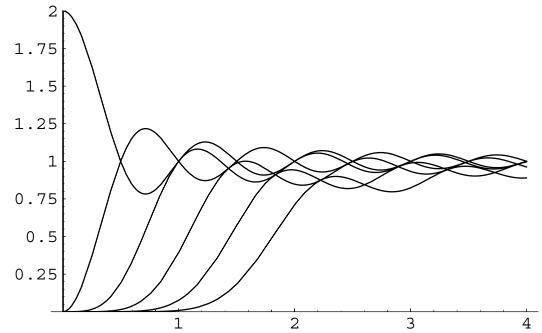

FIGURE 12. The m-hard 1-level edge densities for $m = 0, 1, \ldots, 5$.

to the weight $w(x) = (1-x)^a(1+x)^b$ on $[-1,1]$, the local statistics near the central point $x = +1$ are derived from the asymptotic behavior of these polynomials at the right edge of the interval $[-1,+1]$.[17] More specifically, the relevant kernel that takes the place of the (even or odd) sine kernel is the "edge limit" as $N \to \infty$ of the Christoffel–Darboux/Szegő projection kernel $K_N^{(a,b)}(x,y)$ onto polynomials of degree less than N in $L^2([-1,1],(1-x)^a(1+x)^b dx)$ (via the change of variables (A–17)). For the edge $+1$, the limit depends only on the parameter a and is equal to the Bessel kernel[18]

$$B^{(a)}(\xi,\eta) = \frac{\sqrt{\xi\eta}}{\xi^2-\eta^2}[\pi\xi J_{a+1}(\pi\xi)J_a(\pi\eta) - J_a(\pi\xi)\pi\eta J_{a+1}(\pi\eta)], \tag{A–20}$$

$$B^{(a)}(\xi,\xi) = \frac{\pi}{2}(\pi\xi)[J_a^2(\pi\xi) - J_{a-1}(\pi\xi)J_{a+1}(\pi\xi)], \tag{A–21}$$

where J_ν stands for the Bessel function of the first kind [Nagao and Wadati 91, Dueñez 04].

It is a little more natural for our purposes to use the hardness m, rather than $a = m - \frac{1}{2}$, as the parameter, so we define

$$K^{(m)}(x,y) = B^{(m-1/2)}(x,y), \tag{A–22}$$

$$k^{(m)}(x,y) = \frac{1}{\pi}K^{(m)}(x/\pi, y/\pi). \tag{A–23}$$

Using the recursion formula for Bessel functions we obtain an alternative formula to (A–21) for the diagonal values of the kernel:

$$k^{(m)}(x,x) = \frac{x}{2}[J_{m+\frac{1}{2}}(x)^2 + J_{m-\frac{1}{2}}(x)^2] - \left(m - \frac{1}{2}\right) J_{m+\frac{1}{2}}(x)J_{m-\frac{1}{2}}(x). \tag{A–24}$$

Except for m times a point mass at $x = 0$, the central m-hard 1-level density is given by

$$\rho_m(x) = K^{(m)}(x,x). \tag{A–25}$$

See Figure 12.

A.6 Spacing Measures

In this section we state some well-known formulas giving the spacing measures or "gap probabilities" at the central point. Their derivation is standard and depends only on knowledge of the edge-limiting kernels $K^{(m)}$ (see, for instance, [Katz and Sarnak 99a, Mehta 91, Tracy and Widom 98]). Let $E^{(m)}(k;s)$ be the limit as $N \to \infty$ of the probability that exactly k of the ξ_j's lie on the interval $(0,s)$, where ξ_j is related to x_j via (A–17). Also let $p^{(m)}(k;s)ds$ be the conditional probability that the $(k+1)$st of the ξ_j's to the right of $\xi = 0$ lies in the interval $[s, s+ds)$, in the limit $N \to \infty$.

Abusing notation, let $K^{(m)}|_s$ denote the integral operator on $L^2([0,s],dx)$ with kernel $K^{(m)}(x,y)$:

$$K^{(m)}|_s f(\cdot) = \int_0^s K^{(m)}(\cdot,y)f(y)dy. \tag{A–26}$$

If I denotes the identity operator, then the following formulas hold:

$$E^{(m)}(k;s) = \frac{1}{k!}\frac{\partial^k}{\partial T^k}\det(I + TK^{(m)}|_s)\Big|_{T=-1}, \tag{A–27}$$

$$p^{(m)}(k;s) = -\frac{d}{ds}\sum_{j=0}^{k} E^{(m)}(j;s). \tag{A–28}$$

[17] This "edge limit" and the ensuing Bessel kernels are also observed in the somewhat simpler context of the so-called (unitary) Laguerre ensemble.

[18] In fact, the even sine kernel is given by $S_+ = B^{(-1/2)}$, whereas the odd sine kernel is given by $S_- = B^{(1/2)}$.

On the right-hand side of (A–27), "det" is the Fredholm determinant: for an operator with kernel $\mathcal{K}$,

$$\det(I+\mathcal{K}) = 1+\sum_{n=1}^{\infty}\frac{1}{n!}\int\cdots\int_{\mathbb{R}^n}\det_{n\times n}(\mathcal{K}(x_j,x_k))\,dx_n\cdots dx_1. \tag{A–29}$$

Identical formulas hold even for finite N, provided that the limiting kernel $K^{(m)}$ is replaced by the Christoffel–Darboux/Szegő projection kernel $K_{N-m}^{(m-\frac{1}{2},-\frac{1}{2})}$ associated with the weight $w(x)$ of (A–6) with $a = m-\frac{1}{2}$, acting on $L^2([-1,1],w(x)\,dx)$. In this case, the corresponding operator is of finite rank, the Fredholm determinant agrees with the usual determinant, and the series (A–29) is finite.

A.7 Explicit Kernels

In view of the relation between Bessel functions of the first kind of half-integral parameter and trigonometric functions, it is possible to write the kernels $K^{(m)}$ in terms of elementary functions.

A.7.1 $m = 0$: The Even Sine Kernel.

$$K_0(x,y) = S_+(x,y) = \frac{\sin\pi(x-y)}{\pi(x-y)} + \frac{\sin\pi(x+y)}{\pi(x+y)}. \tag{A–30}$$

The one-level density is

$$\rho_+(x) = S_+(x,x) = 1 + \frac{\sin 2\pi x}{2\pi x}. \tag{A–31}$$

The Fourier transform of the one-level density is

$$\hat{\rho}_+(u) = \delta(u) + \frac{1}{2}I(u), \tag{A–32}$$

where $I(u)$ is the characteristic function of the interval $[-1,1]$.

A.7.2 $m = 1$: The Odd Sine Kernel.

$$K_1(x,y) = S_-(x,y) = \frac{\sin\pi(x-y)}{\pi(x-y)} - \frac{\sin\pi(x+y)}{\pi(x+y)}. \tag{A–33}$$

The one-level density is

$$\rho_-(x) = S_-(x,x) = \delta(x) + 1 - \frac{\sin 2\pi x}{2\pi x}. \tag{A–34}$$

The Fourier transform of the one-level density is

$$\hat{\rho}_-(u) = \delta(u) + 1 - \frac{1}{2}I(u). \tag{A–35}$$

A.7.3 $m = 2$: The "Doubly Hard" Kernel.

$$K_2(x,y) = \frac{\sin\pi(x-y)}{\pi(x-y)} + \frac{\sin\pi(x+y)}{\pi(x+y)} - 2\frac{\sin\pi x}{\pi x}\frac{\sin\pi y}{\pi y}. \tag{A–36}$$

The one-level density is

$$\rho_2(x) = 2\delta(x) + 1 + \frac{\sin 2\pi x}{2\pi x} - 2\left(\frac{\sin\pi x}{\pi x}\right)^2. \tag{A–37}$$

The Fourier transform of the one-level density is

$$\hat{\rho}_2(u) = \delta(u) + 2 + \left(2|u| - \frac{3}{2}\right)I(u). \tag{A–38}$$

A.7.4 $m = 3$: The "Triply Hard" Kernel.

$$K_3(x,y) = K_1(x,y) + \frac{18}{\pi^2 xy}\left(1+\frac{5}{\pi^2 xy}\right)K_0(x,y) - 6\left(\frac{\cos\pi x}{\pi x}\frac{\cos\pi y}{\pi y} + \frac{\sin\pi x}{(\pi x)^2}\frac{\sin\pi y}{(\pi y)^2}\right). \tag{A–39}$$

ACKNOWLEDGMENTS

The program used to calculate the order of vanishing of elliptic-curve L-functions at the central point was written by Jon Hsu, Leo Goldmakher, Stephen Lu, and the author; the program to calculate the first few zeros above the central point in families of elliptic curves is due to Adam O'Brien, Aaron Lint, Atul Pokharel, Michael Rubinstein, and the author. I would like to thank Eduardo Dueñez, Frank Firk, Michael Rosen, Peter Sarnak, Joe Silverman, and Nina Snaith for many enlightening conversations, the referees for a very thorough reading of the paper and suggestions that improved the presentation, and the information technology managers at the Mathematics Departments at Princeton, Ohio State, and Brown Universities for help in getting all the programs to run compatibly.

REFERENCES

[Arms et al. 06] S. Arms, A. Lozano-Robledo, and S. J. Miller. "Constructing Elliptic Curves over $\mathbb{Q}$ with Moderate Rank." Preprint, to appear in *J. Number Theory*, 2006.

[Birch and Swinnerton-Dyer 63] B. Birch and H. P. F. Swinnerton-Dyer. "Notes on Elliptic Curves, I." *J. Reine Angew. Math.* 212 (1963), 7–25.

[Birch and Swinnerton-Dyer 65] B. Birch and H. P. F. Swinnerton-Dyer. "Notes on Elliptic Curves, II." *J. Reine Angew. Math.* 218 (1965), 79–108.

[Breuil et al. 01] C. Breuil, B. Conrad, F. Diamond, and R. Taylor. "On the Modularity of Elliptic Curves over **Q**: Wild 3-adic Exercises." *J. Amer. Math. Soc.* 14:4 (2001), 843–939.

[Brumer 92] A. Brumer. "The Average Rank of Elliptic Curves, I." *Invent. Math.* 109 (1992), 445–472.

[Brumer and McGuinness 91] A. Brumer and O. McGuinness. "The Behaviour of the Mordell–Weil Group of Elliptic Curves." *Bull. AMS* 23 (1991), 375–382.

[Casella and Berger 02] G. Casella and R. Berger. *Statistical Inference*. Second edition. Duxbury Advanced Series, 2002.

[Conrey 05] B. Conrey. "Notes on Eigenvalue Distribution for the Classical Compact Groups." In *Recent Perspectives in Random Matrix Theory and Number Theory*, London Mathematical Society Lecture Note Series, 322, pp. 11–146. Cambridge: Cambridge University Press, 2005.

[Cremona 92] J. Cremona. *Algorithms for Modular Elliptic Curves*. Cambridge: Cambridge University Press, 1992.

[David et al. 04] C. David, J. Fearnley, and H. Kisilevsky. "On the Vanishing of Twisted L-Functions of Elliptic Curves." *Experiment. Math.* 13:2 (2004), 185–198.

[Deift et al. 99] P. Deift, T. Kriecherbauer, K. T.-R. McLaughlin, S. Venakides, and X. Zhou. "Uniform Asymptotics for Polynomials Orthogonal with Respect to Varying Exponential Weights and Applications to Universality Questions in Random Matrix Theory." *Comm. Pure Appl. Math.* 52:11 (1999), 1335–1425.

[Dueñez 04] E. Dueñez. "Random Matrix Ensembles Associated to Compact Symmetric Spaces." *Commun. Math. Phys.* 244 (2004), 29–61.

[Dueñez and Miller 06] E. Dueñez and S. J. Miller. "The Low Lying Zeros of a GL(4) and a GL(6) Family of L-Functions." Preprint available online (http://arxiv.org/pdf/math.NT/0506462), to appear in *Compos. Math.*, 2006.

[Farmer 05] D. Farmer. "Modeling Families of L-Functions." Preprint available online (http://arxiv.org/pdf/math.NT/0511107), 2005.

[Fermigier 92] S. Fermigier. "Zéros des fonctions L de courbes elliptiques." *Experimental Mathematics* 1 (1992), 167–173.

[Fermigier 96] S. Fermigier. "Étude expérimentale du rang de familles de courbes elliptiques sur $\mathbb{Q}$." *Experimental Mathematics* 5 (1996), 119–130.

[Gouvéa and Mazur 91] F. Gouvéa and B. Mazur. "The Square-Free Sieve and the Rank of Elliptic Curves." *J. Amer. Math. Soc.* 4 (1991), 45–65.

[Goldfeld 76] D. Goldfeld. "The Class Number of Quadratic Fields and the Conjectures of Birch and Swinnerton-Dyer." *Ann. Scuola Norm. Sup. Pisa Cl. Sci. (4)* 3:4 (1976), 624–663.

[Goldfeld 79] D. Goldfeld. "Conjectures on Elliptic Curves over Quadratic Fields." In *Number Theory* (Proc. Conf. in Carbondale, 1979), pp. 108–118, Lecture Notes in Mathematics, 751. New York:Springer-Verlag, 1979.

[Gross and Zagier 87] B. Gross and D. Zagier. "Heegner Points and Derivatives of L-Series, II." *Math. Ann.* 278 (1987), 497–562.

[Harvey and Hughes 58] J. A. Harvey and D. J. Hughes. "Spacings of Nuclear Energy Levels." *Phys. Rev.* 109:2 (1958), 471–479.

[Haq et al. 82] R. U. Haq, A. Pandey, and O. Bohigas. "Fluctuation Properties of Nuclear Energy Levels: Do Theory and Experiment Agree?" *Phys. Rev. Lett.* 48 (1982), 1086–1089.

[Heath-Brown 04] R. Heath-Brown. "The Average Analytic Rank of Elliptic Curves." *Duke Math. J.* 122:3 (2004), 591–623.

[Helfgott 04] H. Helfgott. "On the Distribution of Root Numbers in Families of Elliptic Curves." Preprint available online (http://arxiv.org/pdf/math.NT/0408141), 2004.

[Hejhal 94] D. Hejhal. "On the Triple Correlation of Zeros of the Zeta Function." *Internat. Math. Res. Notices* 7 (1994), 294–302.

[Iwaniec et al. 00] H. Iwaniec, W. Luo, and P. Sarnak. "Low Lying Zeros of Families of L-Functions." *Inst. Hautes Études Sci. Publ. Math.* 91 (2000), 55–131.

[Katz and Sarnak 99a] N. Katz and P. Sarnak. *Random Matrices, Frobenius Eigenvalues and Monodromy*, AMS Colloquium Publications, 45. Providence: American Mathematical Society, 1999.

[Katz and Sarnak 99b] N. Katz and P. Sarnak. "Zeros of Zeta Functions and Symmetries." *Bull. AMS* 36 (1999), 1–26.

[Keating and Snaith 00] J. P. Keating and N. C. Snaith. "Random Matrix Theory and $\zeta(1/2+it)$." *Comm. Math. Phys.* 214:1 (2000), 57–89.

[Keating and Snaith 03] J. P. Keating and N. C. Snaith. "Random Matrices and L-Functions." *Random Matrix Theory, J. Phys. A* 36:12 (2003), 2859-2881.

[Mai 93] L. Mai. "The Analytic Rank of a Family of Elliptic Curves." *Canadian Journal of Mathematics* 45 (1993), 847–862.

[McKay 81] B. McKay. "The Expected Eigenvalue Distribution of a Large Regular Graph." *Linear Algebra Appl.* 40 (1981), 203–216.

[Mehta 91] M. Mehta. *Random Matrices*. Second edition. Boston: Academic Press Inc., 1991.

[Mestre 86] J. Mestre. "Formules explicites et minorations de conducteurs de variétés algébriques." *Compositio Mathematica* 58 (1986), 209–232.

[Michel 95] P. Michel. "Rang moyen de familles de courbes elliptiques et lois de Sato–Tate." *Monat. Math.* 120 (1995), 127–136.

[Miller 02] S. J. Miller. "1- and 2-Level Densities for Families of Elliptic Curves: Evidence for the Underlying Group Symmetries." PhD diss., Princeton University, 2002.

[Miller 04] S. J. Miller. "1- and 2-Level Densities for Families of Elliptic Curves: Evidence for the Underlying Group Symmetries." *Compositio Mathematica* 140:4 (2004), 952–992.

[Miller 05] S. J. Miller. "Variation in the Number of Points on Elliptic Curves and Applications to Excess Rank." *C. R. Math. Rep. Acad. Sci. Canada* 27:4 (2005), 111-120.

[Montgomery 73] H. Montgomery. "The Pair Correlation of Zeros of the Zeta Function." In *Analytic Number Theory*, pp. 181–193, Proceedings of Symposia in Pure Mathematics, 24. Providence, American Mathematical Society, 1973.

[Nagao and Wadati 91] T. Nagao and M. Wadati. "Correlation Functions of Random Matrix Ensembles Related to Classical Orthogonal Polynomials." *J. Phys. Soc. Japan* 60:10 (1991), 3298–3322.

[Rosen and Silverman 98] M. Rosen and J. Silverman. "On the Rank of an Elliptic Surface." *Invent. Math.* 133 (1998), 43–67.

[Rubin and Silverberg 01] K. Rubin and A. Silverberg. "Rank Frequencies for Quadratic Twists of Elliptic Curves." *Experimental Mathematics* 10:4 (2001), 559–569.

[Rubinstein 98] M. Rubinstein. "Evidence for a Spectral Interpretation of the Zeros of L-Functions." PhD diss., Princeton University, 1998.

[Rubinstein 01] M. Rubinstein. "Low-Lying Zeros of L-Functions and Random Matrix Theory." *Duke Math. J.* 109 (2001), 147–181.

[Rubinstein 05] M. Rubinstein. "The L-Function Package." Available online (http://www.math.uwaterloo.ca/~mrubinst), 2005.

[Rudnick and Sarnak 96] Z. Rudnick and P. Sarnak. "Zeros of Principal L-Functions and Random Matrix Theory." *Duke Journal of Math.* 81 (1996), 269–322.

[Silverman 86] J. Silverman. *The Arithmetic of Elliptic Curves*, Graduate Texts in Mathematics, 106. New York: Springer-Verlag, 1986.

[Silverman 94] J. Silverman. *Advanced Topics in the Arithmetic of Elliptic Curves*, Graduate Texts in Mathematics, 151. New York: Springer-Verlag, 1994.

[Silverman 98] J. Silverman. "The Average Rank of an Algebraic Family of Elliptic Curves." *J. Reine Angew. Math.* 504 (1998), 227–236.

[Snaith 05] N. Snaith. "Derivatives of Random Matrix Characteristic Polynomials with Applications to Elliptic Curves." *J. Phys. A: Math. Gen.* 38 (2005), 10345–10360.

[Stewart and Top 95] C. Stewart and J. Top. "On Ranks of Twists of Elliptic Curves and Power-Free Values of Binary Forms." *Journal of the American Mathematical Society* 40:4 (1995), 943–973.

[Taylor and Wiles 95] R. Taylor and A. Wiles. "Ring-Theoretic Properties of Certain Hecke Algebras." *Ann. Math.* 141 (1995), 553–572.

[Tracy and Widom 98] C. Tracy and H. Widom. "Correlation Functions, Cluster Functions, and Spacing Distributions for Random Matrices." *J. Statist. Phys.* 92:5, 6 (1998), 809–835.

[Watkins 04] M. Watkins. "Rank Distribution in a Family of Cubic Twists." math.NT/0412427, 2004.

[Wiles 95] A. Wiles. "Modular Elliptic Curves and Fermat's Last Theorem." *Ann. Math.* 141 (1995), 443–551.

[Young 05] M. Young. "Lower Order Terms of the 1-Level Density of Families of Elliptic Curves." *IMRN* 10 (2005), 587–633.

[Young 06] M. Young. "Low-Lying Zeros of Families of Elliptic Curves." *J. Amer. Math. Soc.* 19:1 (2006), 205–250.

[Zagier and Kramarz 87] D. Zagier and G. Kramarz. "Numerical Investigations Related to the L-Series of Certain Elliptic Curves." *J. Indian Math. Soc.* 52 (1987), 51–69.

Steven J. Miller, Department of Mathematics, Brown University, 151 Thayer Street, Providence, RI 02912 (sjmiller@math.brown.edu)

Eduardo Dueñez, Department of Applied Mathematics, University of Texas at San Antonio, 6900 N Loop 1604 W, San Antonio, TX 78249 (eduenez@math.utsa.edu)

Received August 8, 2005; accepted in revised form November 23, 2005.